# MECHANICAL PROPERTIES OF ZIRCONIUM AT ELEVATED TEMPERATURES

by

Knud Borge Pedersen

A Thesis Submitted to the
Graduate Faculty in Partial Fulfillment of
The Requirements for the Degree of
MASTER OF SCIENCE

Major Subject: Nuclear Engineering



Iowa State University
Of Science and Technology
Ames, Iowa

1964

TABLE OF CONTENTS

# LIST OF TABLES

# LIST OF FIGURES

# INTRODUCTION

Zirconium has a low absorption cross section for thermal neutrons, good corrosion resistance at ordinary temperatures, and a high melting point. These properties make it a desirable material for certain structural parts of nuclear reactors (7, pp. 24-25).

Structural materials in nuclear reactors undergo thermal and pressure fluctuations which, because of their frequency, may cause the material to fail; it is therefore desirable to be able to predict the number of cycles of stress to which the material may be subjected at different temperatures without causing failure. The fatigue life of a structural member is normally based on experimental data, frequently presented as an S - N diagram. In order to produce an S - N diagram many specimens are required, each of which is stressed through a maximum and minimum stress repeatedly until the specimen breaks or until some other criterion for failure has been reached. The specimens are stressed to different stress levels, and the results are plotted as stress vs. number of cycles to failure. Because some of the specimens receive many millions of stress reversal the process is time consuming, and any subsequent predictions made from the diagram are valid only for the exact material used for the test specimens and the temperature at which the tests were run. It would be highly advantageous to be able to predict the long-time performance of a material subjected to fluctuating stresses from a few short-time tests.

Some metals, particularly the low carbon steels but also some nonferrous metals, posess a limiting value of stress below which they will not fail if cycled indefinitely. This limiting stress is called the endurance limit. The S - N diagram of such a material will consist of two parts, a curved or sloping line representing stresses above the endurance limit, and a horizontal line representing the endurance limit.

# REVIEW OF THE LITERATURE

The phenomenon of fatigue failure was discovered in the 19th century with the advent of steam-driven machinery. Up to that time the design of structures and machines was based on the static properties of the materials involved, and usually a large factor of safety was employed.

With the faster speeds developed in rotating machinery vibrations and cyclic loads were encountered which sometimes resulted in unexpected failures. The failures were even more surprising in that ductile materials exhibited brittle fractures.

Since the first discovery of fatigue failures much effort has been spent and large amounts of data have been collected in an effort to understand better the phenomenon of fatigue, and to try to eliminate its occurrence.

Extensive research on fatigue was undertaken on railway equipment about forty years ago. Increased attention has been directed to fatigue more recently because of the increasing importance of the airplane. Optimum design is paramount for aircraft and this means reduction in size and weight of the component parts. The early designers had little experience with the vibrations that could be caused by the high speed movement through the air, and consequently many fatigue failures occurred.

Today fatigue failures may be expected in all types of machinery and structures due to the fact that machines move faster and that many structures carry vibrating machinery.

Many theories exist on fatigue, using various simplifying assumptions; however, due to the complexities of the phenomenon none of the theories serves as a direct tool to prevent fatigue failure in the design of structures. Orowan (12) proposed a model consisting of an elastic matrix surrounding a "plastic inhomogeneiety". This inhomogeneiety could be a fault or a crystallite which was unfavorably oriented with respect to an applied load, so that its yield point would be exceeded by a stress which would only produce elastic strains in the surrounding material. Orowan considered two effects to be caused by repeated application of plastic deformation to this region: 1) Deformation which may be cumulative under succeeding cycles until a self-propagating crack is formed, and 2) local strain hardening and corresponding stress relief which strengthens the region and shifts stress maxima to adjacent material. By making simplifying assumptions concerning these effects Orowan was able to explain semiquantitatively many of the observed phenomena of fatigue behavior of metals.

Machlin (10) suggested a theory which explained the development of plastic deformation by the growth and spread of dislocations in the crystalline structure of the metal.

Grover et al. (5, pp. 16-17) found that the progress of fatigue occurs in three stages: 1) the start of a crack spreading out from some nucleus, 2) propagation of the crack under successive cycles of loading, and 3) final rupture when the crack has weakened the section.

They also reported that considerable effort has been expended to correlate fatigue strength of metals with other engineering properties such as static tensile strength, yield strength, proportional limit, creep - rupture strength, etc., and that for some materials there appears to be some correlation between fatigue strength and static tensile strength, but that most of the other attempts were unsuccessful.

Coffin and Read (4) described a softening process which occured when cold-worked metals were subjected to cyclic loading. In order to explain it they used Mott's (11) concept of strain hardening based on the blocking effect of dislocations at grain boundaries and other sources of interference. They considered a cold-worked structure with numerous slip planes and piled up dislocations at the ends of these planes; subsequent strain cycling, where the strains were small relative to the prior deformation was envisaged as a device for relieving the blocking effect of the dislocations. The relief was brought about by permitting the dislocations previously generated to move back and forth along slip planes so that dislocations of opposite sign were permitted to combine and cancel one another. The rate of recombination and redistribution of the dislocation decreases with time.

Coffin (3) found that the fatigue resistance of cold-worked materials under strain cycling conditions may be greater or less than that for the same material in the annealed state, depending

on the magnitude of the strain range. The softening was due to the high strain rate employed initially.

Coffin and Read concluded that a mechanism of failure such as that proposed by Orowan and others in which failure was attributed to a limit of the strain-hardening process was not consistent with experimental fact as obtained by them.

Polakowski and Palchoudhuri (14) similarly found that initially hard-drawn metals showed a softening when they were cycled, whereas the same metals in the soft-annealed state with the application of similar treatment invariably resulted in strain hardening.

Irrespective of whether the metal was initially annealed or cold-worked the change in the static stress - strain properties was the more pronounced the larger the number of cycles applied and the higher the cyclic amplitude. Of the two factors the amplitude was the more potent.

The results indicated that initially cold-worked metals showed a distinct overall softening under fatigue loads. It was suggested that a fatigue fracture is originated as a result of the gradual breakdown under cyclic strain of the initially high elastic, or quasi-elastic, properties acquired by the metal as the result of initial cold-working. Consequently the plastic component of the cycle increases gradually instead of being attenuated. Under these circumstances, they found, the initiation of the fatigue crack is associated not with the exhaustion of the ductility (or plasticity) by progressive work hardening

but rather with the semiplastic condition developed by the action of the alternating strains.

Strain aging was reported by Rally and Sinclair (15) to be a factor in the occurence of the "knee" in the S - N diagram. They also found the shape of the S - N diagram influenced by strain aging which occured during the test, and investigated the variation in position of the knee with temperature.

By removing part of the elements associated with strain aging from the metal they shifted the knee to a longer life and theorized that complete removal of the elements would eliminate the knee altogether so that the metal would no longer exhibit an endurance limit. Raising or lowering the temperature severely also shifted the knee to a longer life.

Quantitative prediction on the location of the knee could not be made because the relationship between temperature and rate of crack propagation is unknown.

According to their report a metal which is susceptible to strain aging to the extent that it exhibits a yield point in a static tensile test should exhibit a knee in the S - N diagram within a limited temperature and cyclic frequency range. However, the knee position would not be a specific point but subject to scatter.

It should be noticed that Rally and Sinclair were concerned not with strain hardening but with strain aging. The former is found in any metal which is strained even a small amount, whereas for a metal to be susceptible to strain aging it must

contain certain alloying elements and may have to be strained severely or repeatedly before there is a change in properties.

Wheeler and Gordon (17, pp. 1-5) in their work with copper showed that the effect of superimposing a 5 per cent compressional deformation on a 30 per cent elongation increased the total stored energy in the sample by reducing the amount released during recrystallization, but increased the amount released during the recovery period by a larger amount. They concluded that reversed deformation which produces a work softening appears to increase the amount of stored energy, and explained in terms of structural imperfections that reversed deformation may produce new defects in the lattice and in addition rearrange those already present in such a manner that many more of the defects are annealed out in recovery.

Swindeman and Douglas (16) investigated the effects of frequency and grain size on the fatigue life of Inconel, and also compared thermal strain cycling data with strain cycling data obtained at the same mean temperature.

They found that good correlation existed between the two types of data, and that the typical equation for strain cycling $N^{\alpha} \epsilon_p = K$, where N is the number of cycles to failure, $\epsilon_p$ is the plastic strain per cycle, and $\alpha$ and K are constants, held for thermal strain cycling. Both grain size and frequency were found to have a pronounced effect on the rupture life at higher temperatures with fine grained materials surviving more cycles before failure than coarse grained material, and with long time

cycles shortening the number of cycles to failure when the strain per cycle was low.

Kearns and Mudge (8) conducted an investigation to find the factor responsible for the different values of notch sensitivity in crystal bar - tin and sponge - tin - zirconium alloys. Since oxygen is the principal difference in the composition of the two they were particularly interested to see whether or not the oxygen content influenced the notch sensitivity.

They found that a higher temperature in addition to lowering the effect of stress concentration also lowered the absolute fatigue strength, but raised the fatigue ratio (unnotched fatigue strength/tensile strength).

The addition to zirconium of tin, oxygen, or both increased the unnotched fatigue strength but had considerably less effect on the notched fatigue strength.

They found that the unnotched fatigue strength varies according to the tensile strength whereas the notched fatigue strength remains essentially unchanged. From this they concluded that little can be gained by increasing the strength of zirconium if in service it is to be subjected to fatigue loading in the presence of severe stress raisers.

The effect of oxygen on the fatigue properties of zirconium appeared to be the same as the effect of other elements which increase the tensile strength to the same degree. The fact that notch sensitivity of the oxygen alloy was found to decrease markedly with temperature increase was not considered

unreasonable in view of the fact that the tensile strength also decreased appreciably.

Notch sensitivity was found to be decidedly reduced at high stresses and in the case of unalloyed zirconium the strength of a notched specimen might be higher than that of an unnotched one if stressed sufficiently high to cause failure within the range of $10^4$ to $10^5$ cycles.

They found it noteworthy that zirconium and also titanium exhibit a knee in the S - N curve since this is uncommon to most non-ferrous metals, but is a characteristic of materials which exhibit a tensile yield point such as steel. They also found that with respect to the fatigue ratio zirconium is comparable to steel, having a higher ratio than most non-ferrous metals. They concluded that these properties of zirconium are due to strain aging.

## OBJECTIVES OF THE INVESTIGATION

Since little information is available on the variation of the mechanical properties of zirconium with temperature this investigation was undertaken primarily to evaluate the properties.

The ultimate tensile strength, the yield strength at 0.2% offset, the modulus of elasticity, and the proportional limit were determined from tensile tests, and the endurance limit and the S - N diagram were determined from fatigue tests. All of the properties were evaluated at various temperatures for three different preparations of zirconium.

A second objective of the investigation was to explore methods which might be used for evaluating the endurance limit for zirconium without the time-consuming tests normally employed.

## MATERIAL

Three different types of zirconium were used in the investigation, (1) swaged iodide zirconium, (2) electron-beam melted iodide zirconium, and (3) sponge zirconium.

The iodide zirconium was received as 5/8 inch diameter crystal bars which were swaged at room temperature down to 0.575 inch diameter, a 15% reduction in area. The swaged bars were annealed by heating at the rate of 30 C per hour up to 600 C at which temperature they were held for 24 hours before cooling at the rate of 100 C per hour. Photomicrographs taken after the annealing showed no evidence of strains.

Some of the iodide zirconium was electron-beam melted into 1 3/4 inch diameter billets 4 inches long which were rolled and swaged at room temperature to 5/8 inch diameter, an 87% reduction in area; they were then annealed for two hours at 900 C with furnace cooling, giving them the same apparent grain structure as the swaged and annealed iodide zirconium.

It was assumed that there would be little difference in the chemical compositions of the two iodide zirconiums, and the beam melting was carried out in order to eliminate any inhomogeneities that might have been present in the swaged and annealed material.

The sponge zirconium was received as a 5 1/2 inch diameter evaluation ingot approximately 9 inches long. The ingot was cut into 4 inch long 1/2 inch square specimen blanks, which were numbered according to their original position in the ingot.

The intention was to make the tests on the as-received material without any previous annealing. In order to make sure that the ingot was substantially homogeneous, hardness tests were taken at each end of all of the blanks. The average hardness value was 43.5 Rockwell "A" with a standard deviation of 2.1 Rockwell "A" but the variation was completely random throughout the ingot.

Chemical and spectrographic analyses for the three materials are shown in Table 1 , with only a chemical test performed on the beam-melted iodide zirconium to see whether or not the oxygen content had changed in the melting operation. Photomicrographs of the three materials appear in Figure 1.

TABLE 1. Chemical and Spectrographic Analyses

| Element | Concentration in sponge Zr, ppm | Concentration in iodide Zr, ppm | Concentration in beam-melted iodide Zr, ppm |
|---|---|---|---|
| Al | < 35 | 30 | |
| B | < 0.2 | - | |
| C | 80 | 100 | |
| Cd | < 0.2 | - | |
| Co | < 10 | - | |
| Cr | < 25 | < 20 | |
| Cu | 25 | < 20 | |
| Fe | 560 | ~ 100 | |
| Hf | 80 | < 1000 | |
| Mg | < 10 | < 20 | |
| Mn | < 25 | FT* | |
| Mo | < 20 | FT | |
| Na | 270 | FT | |
| Ni | 20 | < 50 | |
| Pb | < 20 | - | |
| Si | 40 | ~ 100 | |
| Ti | < 20 | < 25 | |
| U | 0.24 | - | |
| W | < 20 | - | |
| O | 1290 | < 30 | ~ 90 |
| H | - | 50 | 34 |
| N | 40 | 38 | 30 |

* FT = Faint trace.

a)

b)

c)

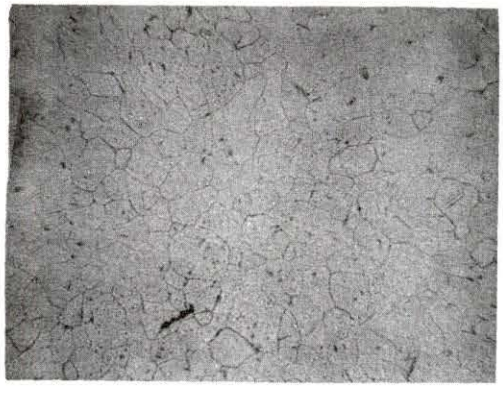

Fig. 1. As-tested materials. Magnification 50 x

a) Sponge-source Zr showing "Windmanstatten" structure indicating moderately rapid cooling

b) Swaged crystal-bar Zr slowly cooled from 600 C

c) Beam melted crystal-bar Zr furnace cooled from 900 C

# EXPERIMENTAL PROCEDURE

## Specimens

The specimens were prepared by machining the material to the dimensions shown in Figure 2. The fatigue specimens were polished, finishing with 0.3 $\mu$ synthetic sapphire. During the polishing operation the specimen and the polishing wheel were both rotated with their axes at a 90-degree angle at speeds such that the abrasive was incident at approximately 45 degrees to the center line of the specimen (13, pp. 8-9). The tensile specimens were not polished prior to testing.

## Equipment

### Fatigue

The fatigue machines were all of the simply supported rotating beam type with a motor driving each end of the specimen to eliminate torsional loads. The ends of the specimen were free to travel in the axial direction, to eliminate shear loads along the test section. Marshall furnace controllers regulated the temperature in the split type Multiple Unit furnaces to within $\pm 2$ C.

The number of cycles to failure were recorded on a revolution counter which indicated every 100 revolutions of the specimen and which shut off with the motors at the instant of failure.

In order to protect the specimens from atmospheric corrosion each was capsulated in a type 310 stainless steel tube with a bellows around the test section to allow flexure. The capsule

was welded around the specimen inside a chamber filled with argon, providing an inert atmosphere inside the capsule and supporting the arc during the welding operation. The capsulation procedure of the specimens was described by Bohn (1, pp. 39-40) and is illustrated in Figure 3.

Tensile

The tensile machine was a 60,000-lb Baldwin-Southwark hydraulic unit which was modified to provide a low-pressure, high-temperature atmosphere around the tensile specimen. A pressure as low as $1 \times 10^{-6}$ mm Hg could be maintained, and the temperature could be varied up to 900 C.

A linear variable differential transformer (LVDT) transferred the strain readings from the knife edges to the x-axis of a Mosley Autograf recorder and another LVDT connected to the Tate-Emery load indicator transferred the load readings to the y-axis of the recorder, thus yielding directly a curve of load vs. strain (2).

## Testing Procedure

Fatigue

The fatigue machines were calibrated for the test temperatures by placing a thermocouple next to a bare specimen while it rotated inside the furnace. A Brown strip-chart recorder was connected to the thermocouple and the machine was left running for a 12-hour period after the test temperature had been

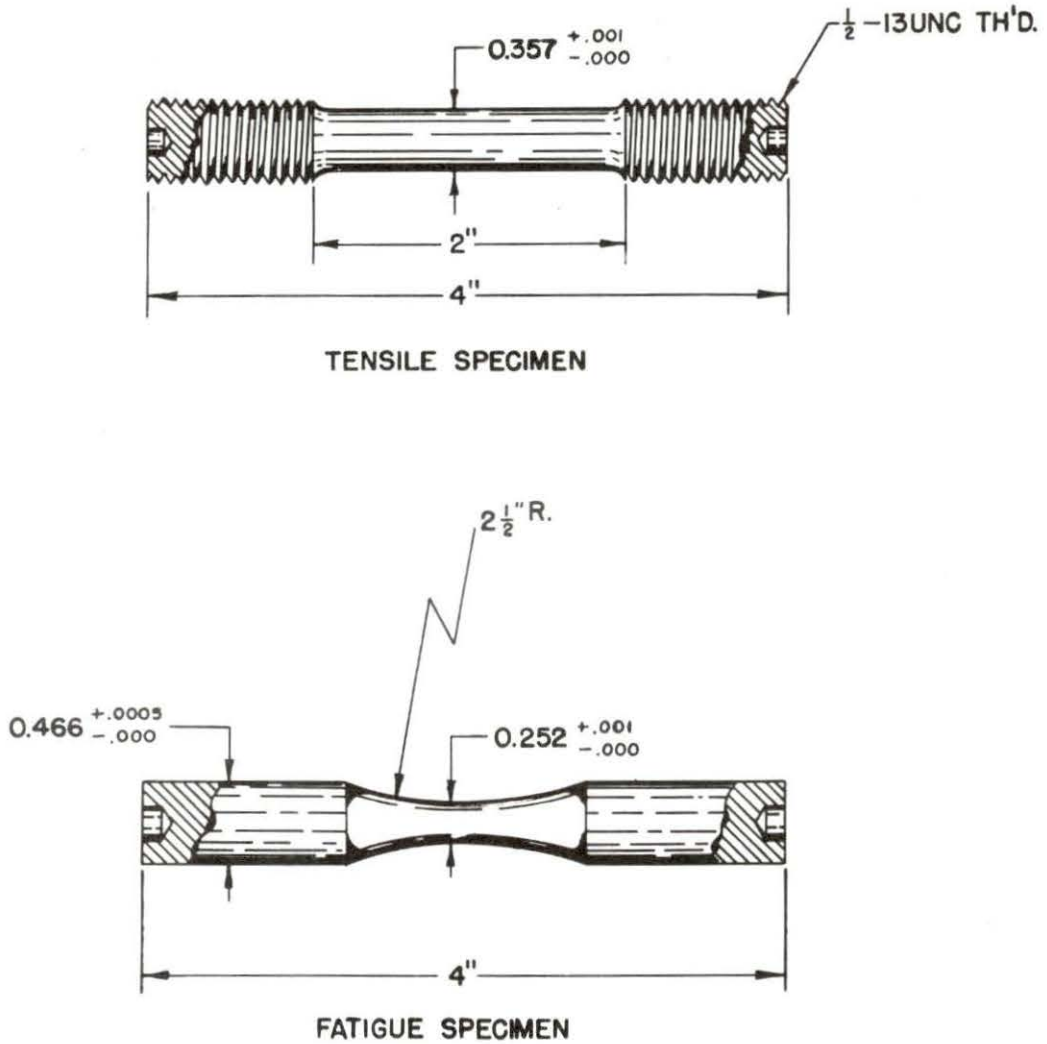


Fig. 2. Specimen dimensions

a)

b)

c)

d)

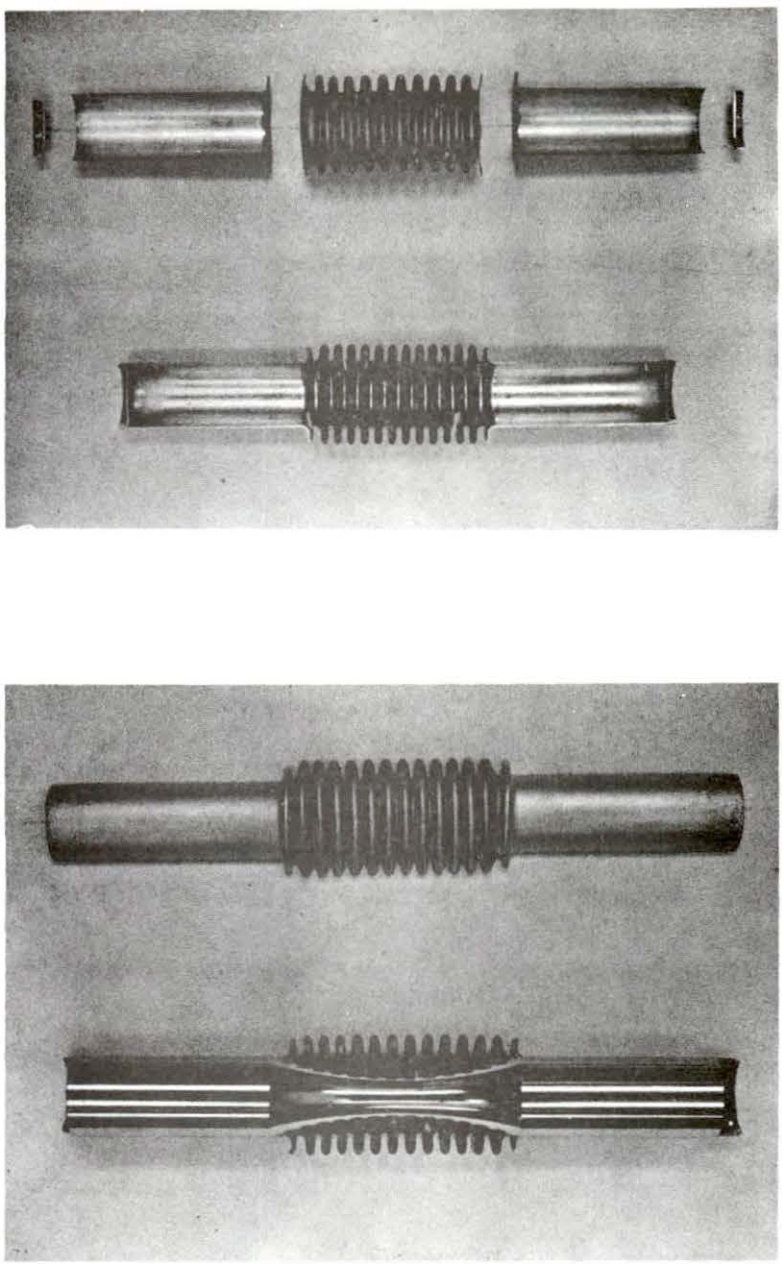

Fig. 3. Capsulation of fatigue specimens.

a) Exploded view of capsule

b) Cross-section of empty capsule

c) Assembled capsule

d) Cross-section of capsule with specimen

attained, in order to observe the temperature fluctuations that might take place due to changes in room temperature and circuit loads. The specimen temperature was not found to deviate from the mean by more than 2 C.

The machines were balanced by placing two specimen halves in the grips, then starting the two motors, and adding or subtracting lead shot in the load pans until the specimen halves were aligned when viewed through a telescope. This procedure eliminated any moment on the specimens due to the weight of the structural members and the specimen itself.

Each motor was calibrated to 4500 rpm by using a stroboscope. A fatigue test was performed by placing a capsulated fatigue specimen in the grips and then starting the motors and furnace. The reason for starting the motors before the test temperature was reached was that the temperature calibration was done with a rotating specimen and it was found that starting the motors after the test temperature had been reached cooled the specimen by several degrees by setting convection currents in motion. It was also felt that the initial start-up might place a load on the specimen which could cause structural damage at a high test temperature.

When equilibrium conditions had been reached the revolution counter was set in such a manner that 10 additional revolutions of the counter would cause it to read zero. These 10 revolutions were used as a count-down for placing the weights

on the pans. When the specimen failed, a micro-switch activated by the beam deflection turned off all power to the machine.

Tensile

The tensile specimen was placed inside the test chamber and the knife edges and thermocouples attached. The chamber was then hung from the moving cross-head of the tensile machine through a furnace and connected to the vacuum system. The system was pumped down to a pressure of $5 \times 10^{-6}$ mm Hg and the furnace controller turned on. The temperature of the furnace was observed on a Brown circular recorder and controlled electronically; thermocouple readings taken in four different positions along the 1 1/2 inch gage length were read on Wheatstone bridges.

## Calculations

The resisting moment of the stainless-steel capsule covering the fatigue specimen was evaluated at room temperature by suspending an empty capsule as a cantilever and finding the deflection as a function of load. The ratio of the resisting moments of the capsule and the specimen was then calculated for all test temperatures by using the appropriate values for the moduli of elasticity. The ratio varied from 0.026% at 150 C to 0.05% at 750 C and was considered sufficiently small to be neglected.

The tensile stress which resulted from the expansion of the argon gas in the capsule under high temperature was calculated

to be 144 psi for a temperature change from 25 C to 750 C and was neglected.

The stress caused by the bending moment on the fatigue specimen was calculated by using the conventional formula $S = \frac{Mc}{I}$. Although this formula is valid only in the proportional range of stress, it was applied in the non-proportional range for purposes of comparison. Figure 4 shows four stress-strain curves of zirconium at 750 C. One of the curves is from an ordinary tensile test, whereas the other three are from flexural tests. The static bending curve falls close to the tensile test curve, and if sufficient points had been established they would probably coincide.

The dynamic bending tests appear much higher, in fact for 80 cycles per second which is near the rate at which the fatigue tests were carried out, the proportional limit is much higher than the ultimate tensile strength as obtained from the ordinary tensile test. This shows that the strength of zirconium at elevated temperatures is rate dependent (9, pp. 491-499), and also that the flexure formula gives reasonable values for comparison of the stresses used in the fatigue tests.

The S - N diagrams were made from least-square fitting of the fatigue data. The curves were assumed to be straight lines on log paper with the resulting equation of the form $\ln S = m \ln N + \ln b$, where S is the stress in psi, N is the number of cycles to failure, m is the slope and b is the intercept, at N = 1, in psi. When the slopes and intercepts had been

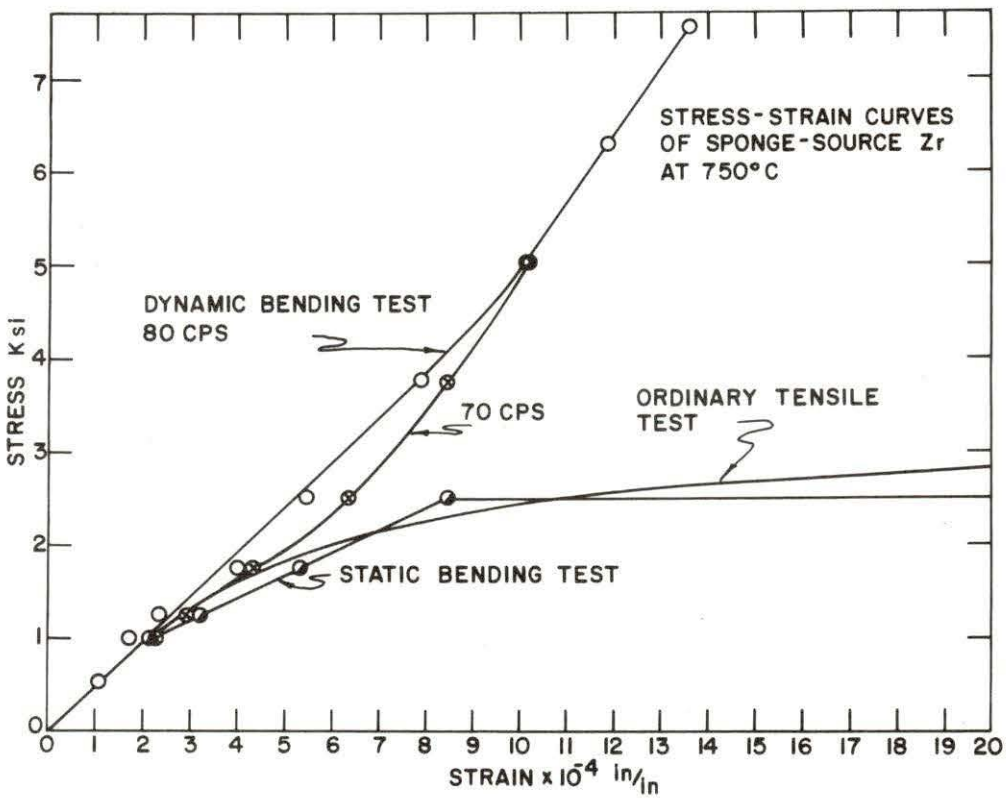


Fig. 4. Stress-strain curves of sponge-source Zr at 750 C

established they were plotted as functions of temperature.

The modulus of elasticity was found by cyclic tensile loading. As a result of strain hardening the proportional limit increases for the first load applications until it attains a constant value.

Several load applications were made after the limiting proportional limit had been reached, and the modulus of elasticity was determined as the average of the slopes of the stress-strain diagrams for these tests.

## RESULTS

The results of the fatigue tests are presented as S - N curves in Figure 5 for the sponge-source zirconium, in Figure 6 for the swaged and annealed iodide zirconium, and in Figure 7 for the beam-melted iodide zirconium. Fatigue tests of the beam-melted iodide zirconium were only performed at 150 C and 450 C due to the limited number of specimens available. The intercepts and slopes of all of those curves are plotted as functions of temperature in Figure 8 and the endurance limits as functions of temperature in Figure 9. The intersection of the sloping part of the S - N curve with the endurance limit (the knee) occurs at a number of cycles dependent on the temperature; this is shown in Figure 10.

Stress-strain diagrams resulting from tests at several temperatures are plotted in Figures 11 through 13 for the three materials, with an original recording of a room temperature tensile test shown in Figure 14.

Figure 15 is a reproduction of the chart obtained in a series of tensile loadings taken in rapid sequence. The curves show that the effect of a series of repeated loadings is to decrease the modulus of elasticity and to increase the proportional limit through the strain hardening effect.

Figures 16 through 20 show various tensile properties plotted as functions of temperature.

Table 2 lists fatigue and tensile properties of the three materials at different temperatures. The two columns headed

"Intercept" and "Slope" are for the empirical equations describing the S - N curves which are of the form $\ln S = m \ln N + \ln b$. Where $\ln b$ is the intercept and m is the slope.

Fatigue properties are plotted as functions of tensile properties in Figures 21 and 22. Figure 21 may also be expressed as $S_{1/2} = 5.49 \ln S_t + 12.41$, where $S_{1/2}$ is the half-cycle intercept expressed in ksi and $S_t$ is the tensile strength in ksi.

Figures 23 and 24 show S - N curves. Those at temperatures up to 450 C were obtained using the proportional limit as found from cyclic tensile tests instead of the endurance limit, the half-cycle intercept as determined by Figure 21, and the occurrence of the knee from Figure 10. Super-imposed on the curves are the points representing the fatigue tests, and it appears that there is good agreement.

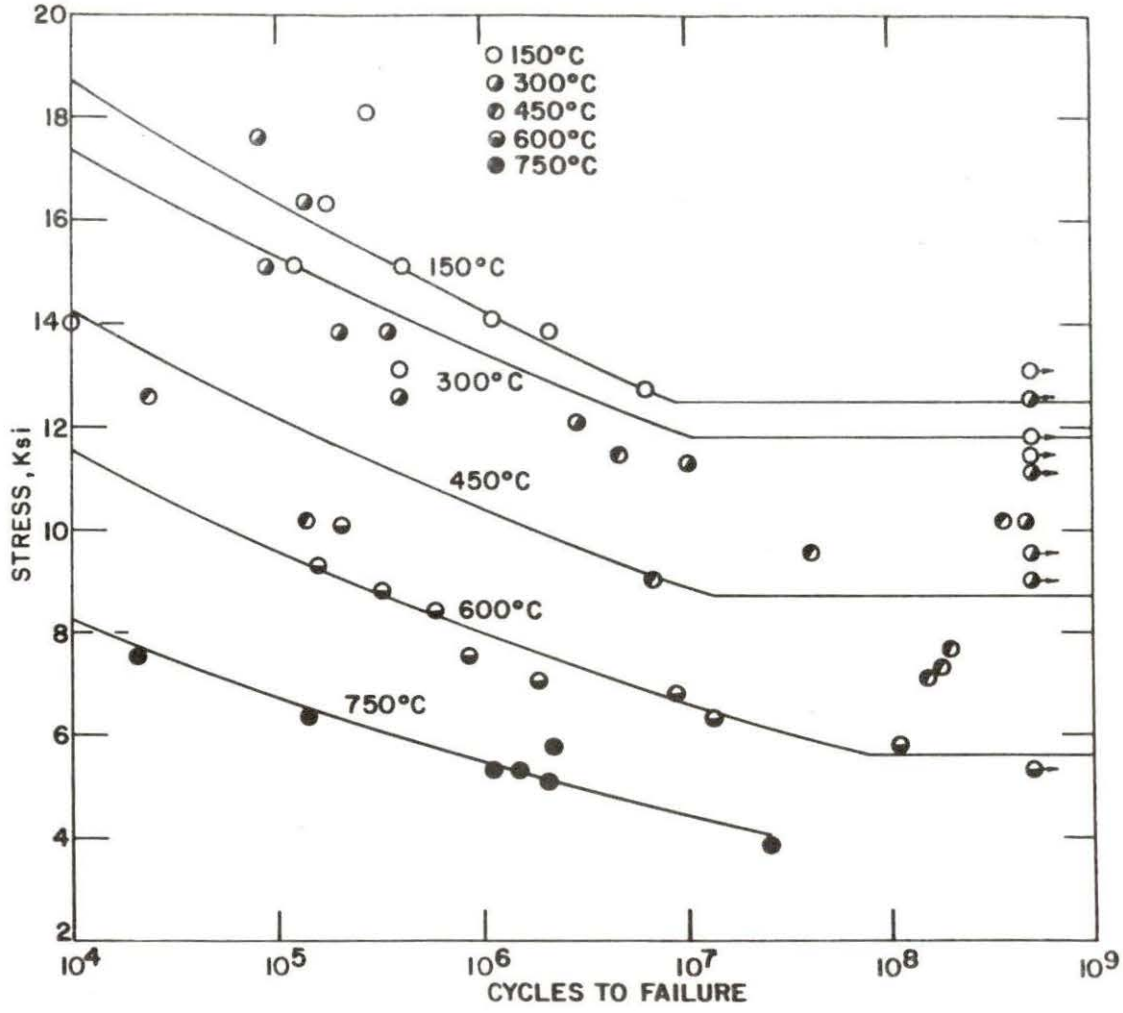


Fig. 5. S - N curves of sponge zirconium.

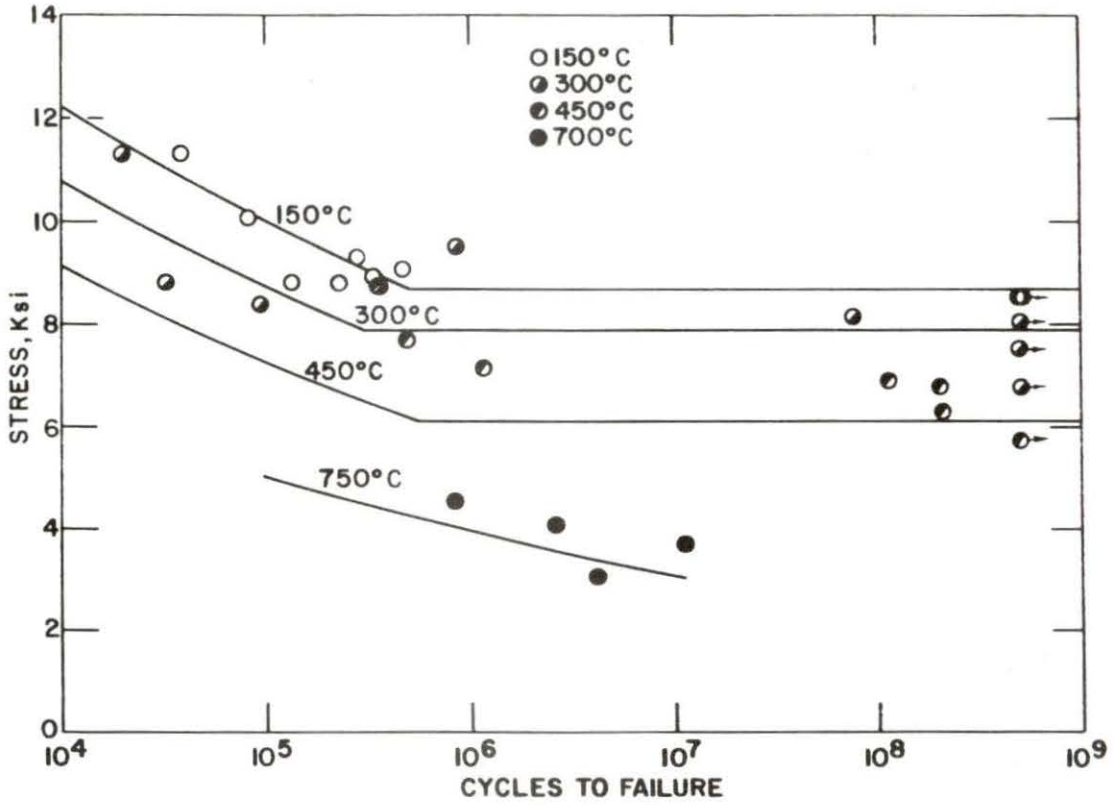


Fig. 6. S - N curves of swaged and annealed iodide zirconium

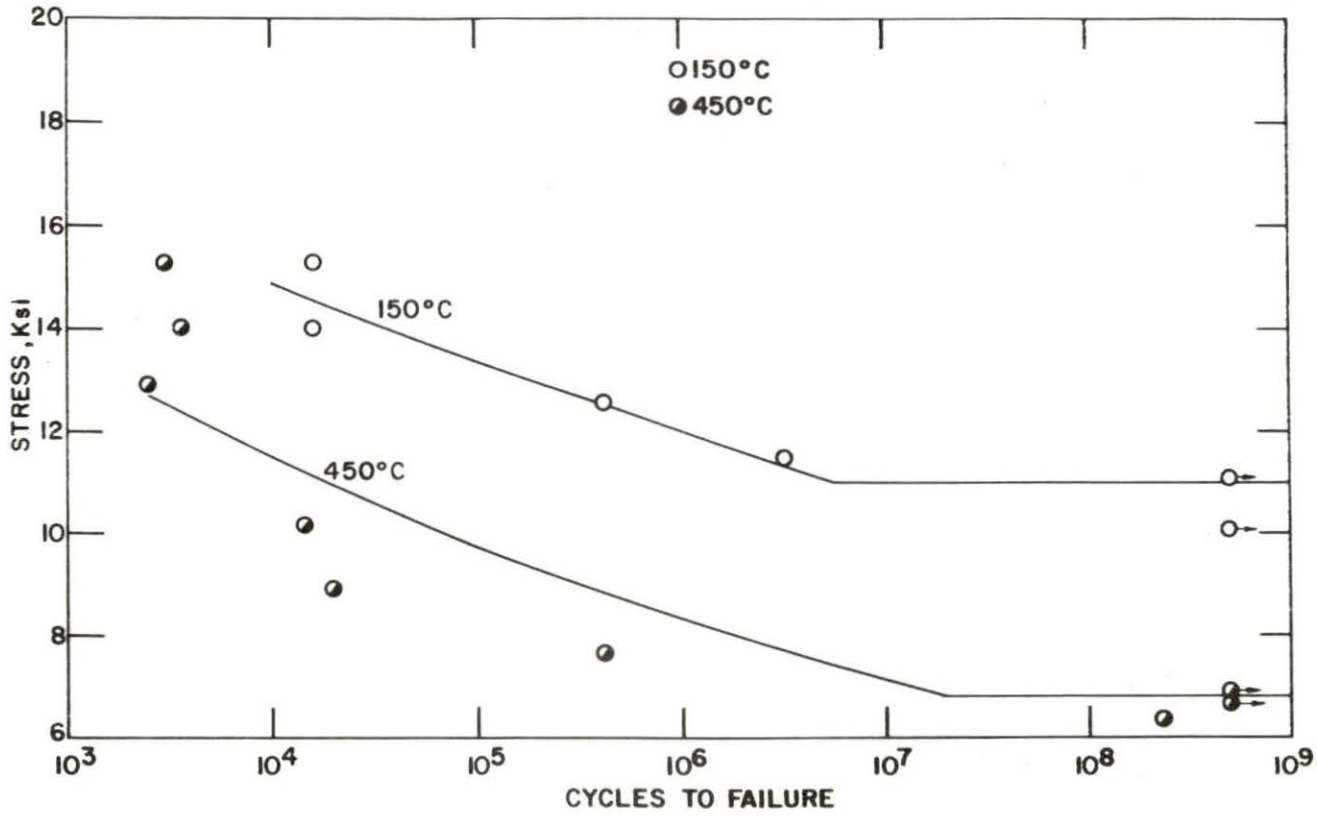


Fig. 7. S - N curves of beam-melted iodide zirconium

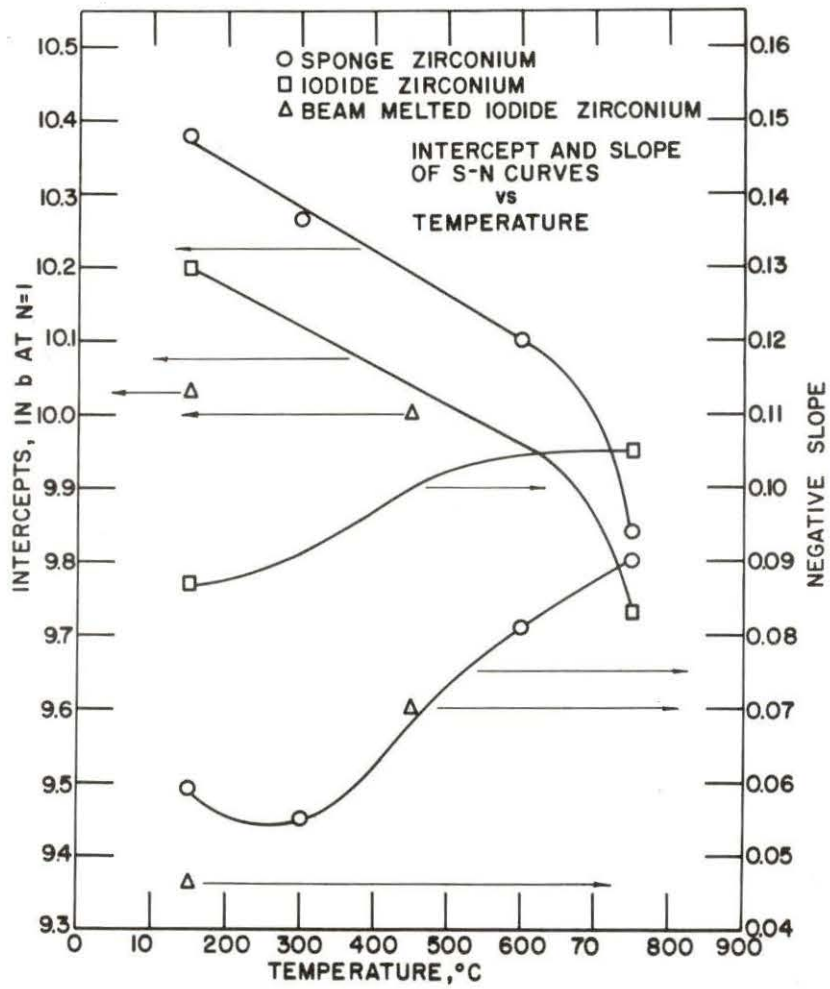


Fig. 8. Intercept and slope of S - N curves vs. temperature

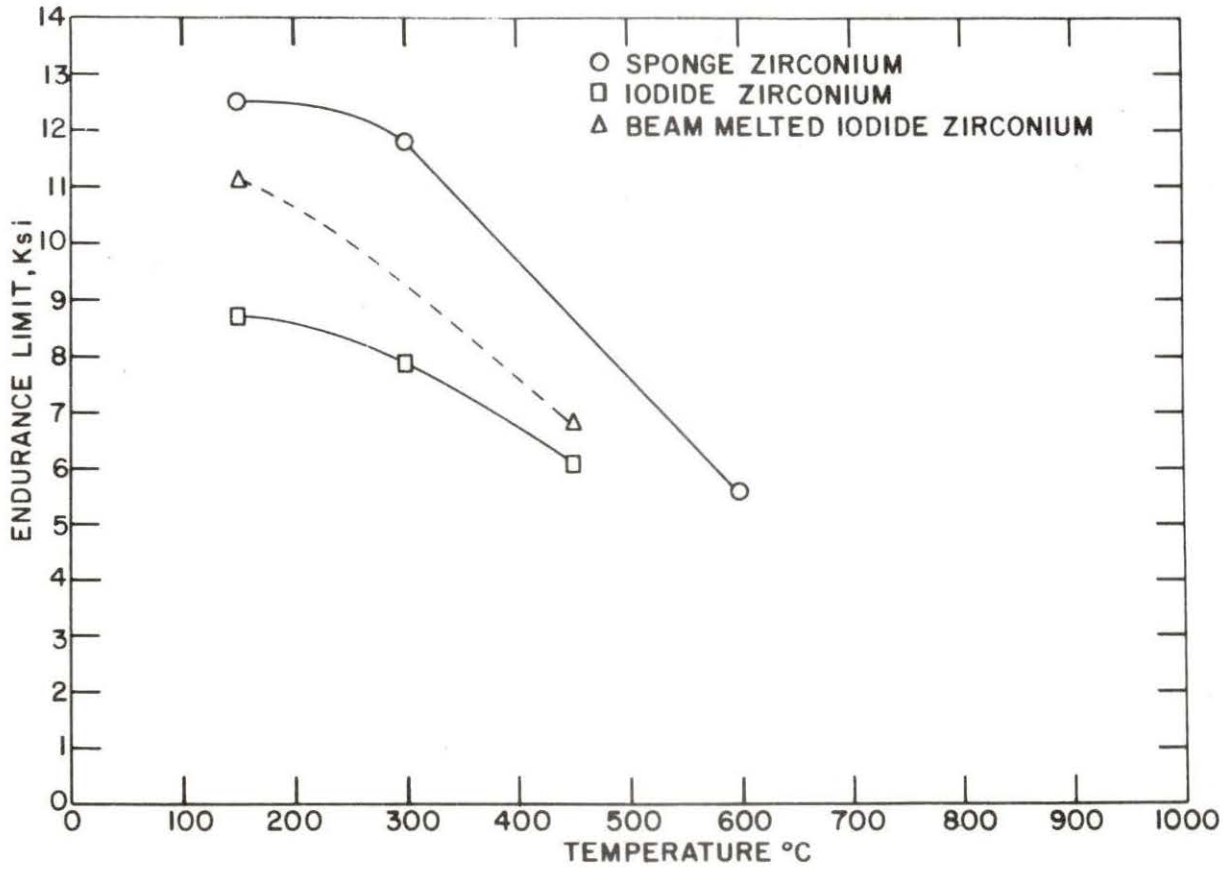


Fig. 9. Endurance limit vs. temperature for three types of zirconium

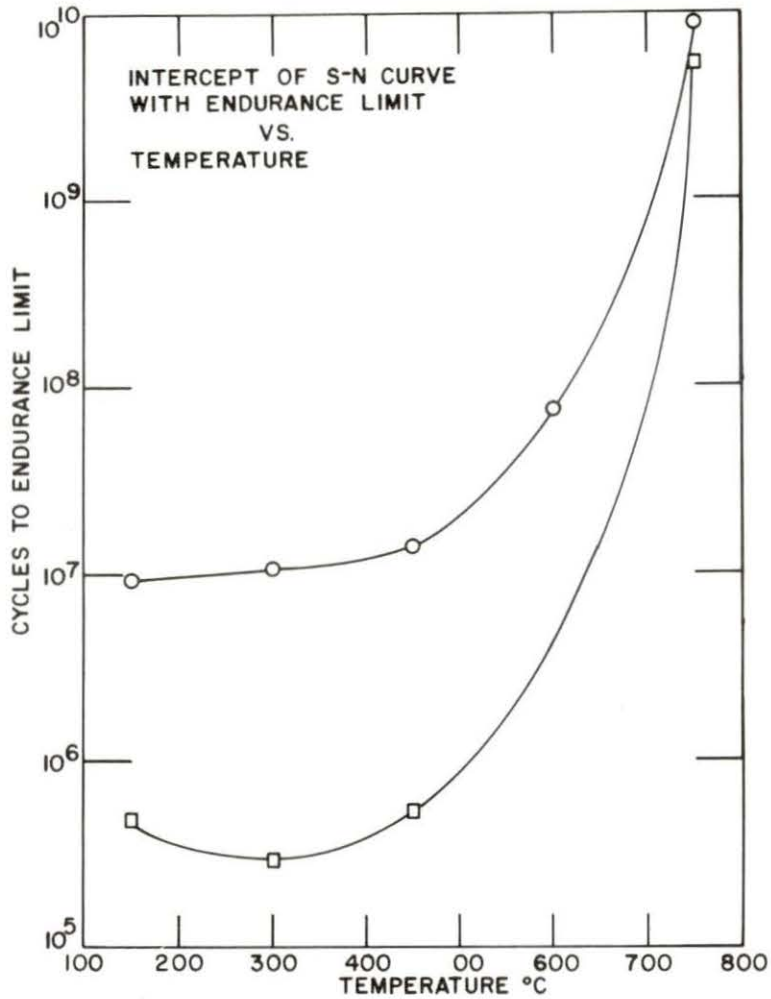


Fig. 10. Intercept of S - N curve with endurance limit vs. temperature

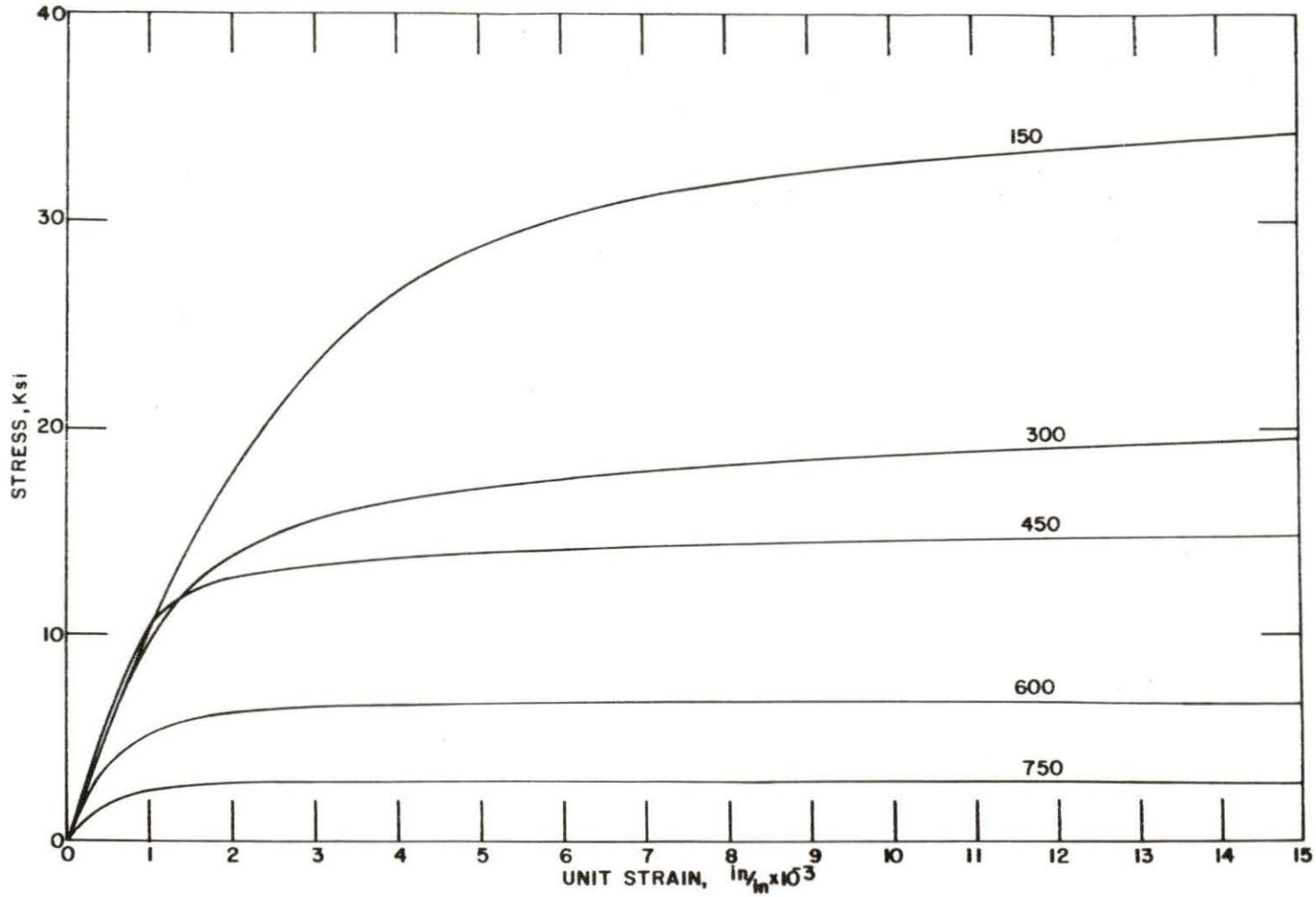


Fig. 11. Stress-strain diagrams for sponge zirconium

Specimen diameter 0.357 in.
Gage length 1.5 in.
Strain rate 0.025 in./in. min.$^{-1}$

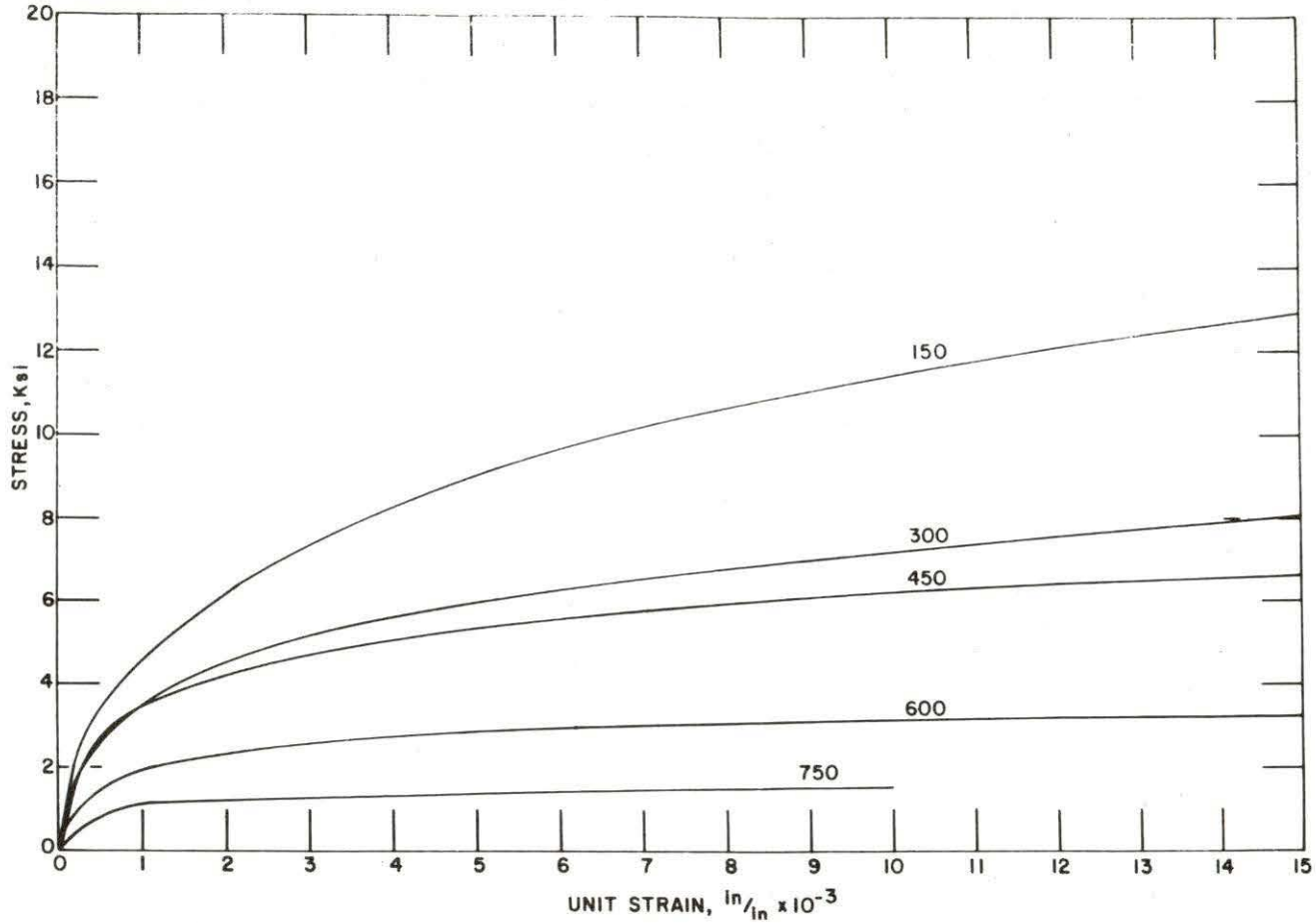


Fig. 12. Stress-strain diagrams for swaged and annealed iodide zirconium

Specimen diameter 0.357 in.
Gage length 1.5 in.
Strain rate 0.025 in./in. min.$^{-1}$

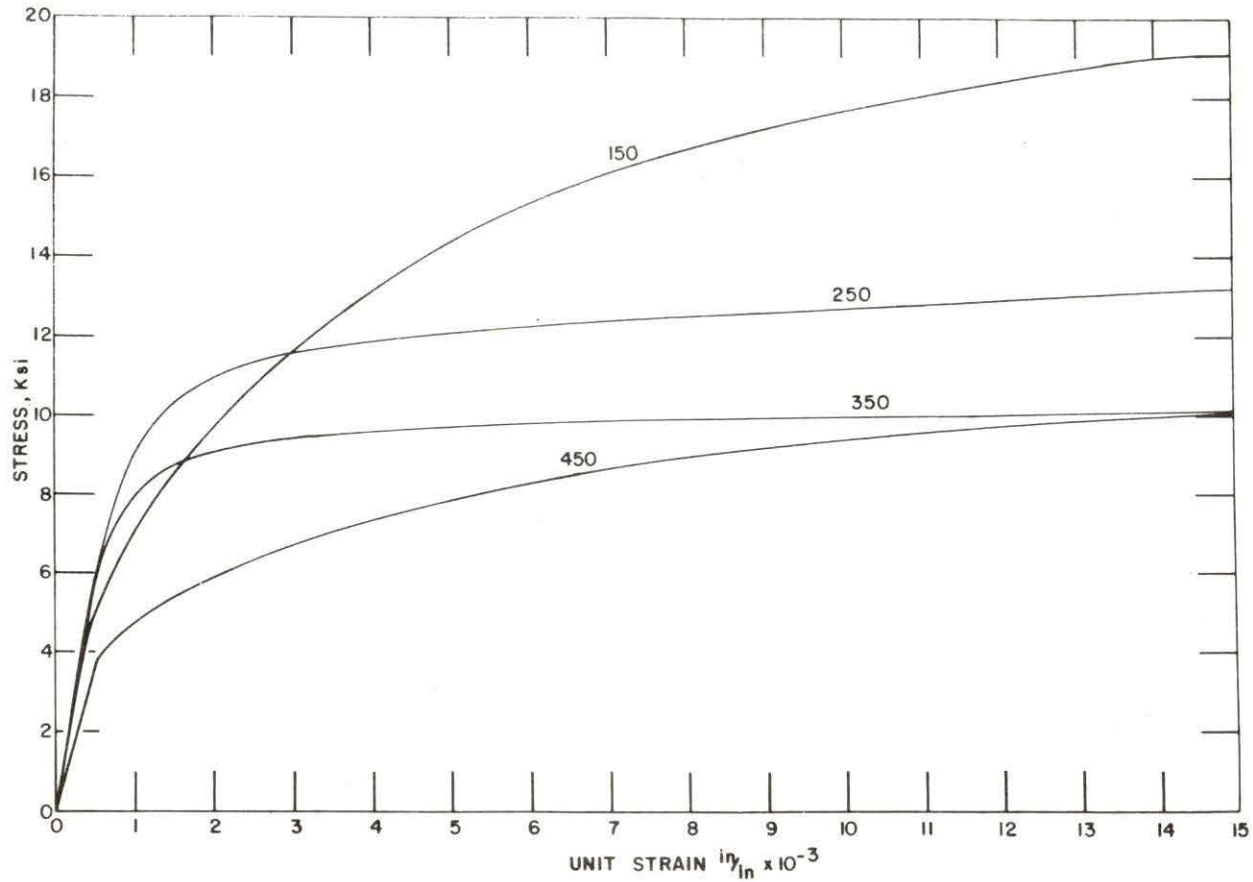


Fig. 13. Stress-strain diagrams for beam-melted iodide zirconium

Specimen diameter 0.357 in.
Gage length 1.5 in.
Strain rate 0.025 in./in. min.$^{-1}$

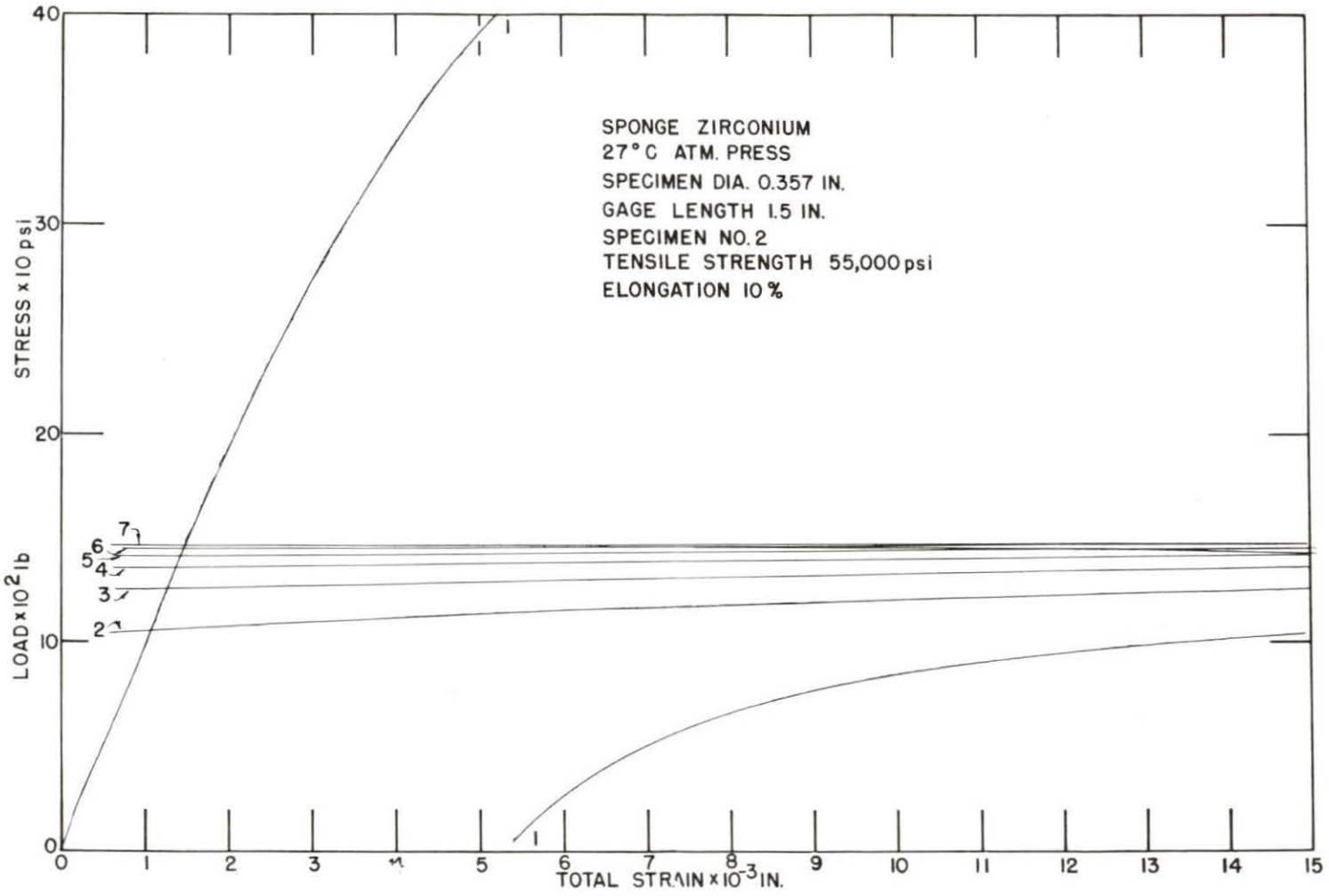


Fig. 14. Recording of room-temperature tensile test of sponge zirconium

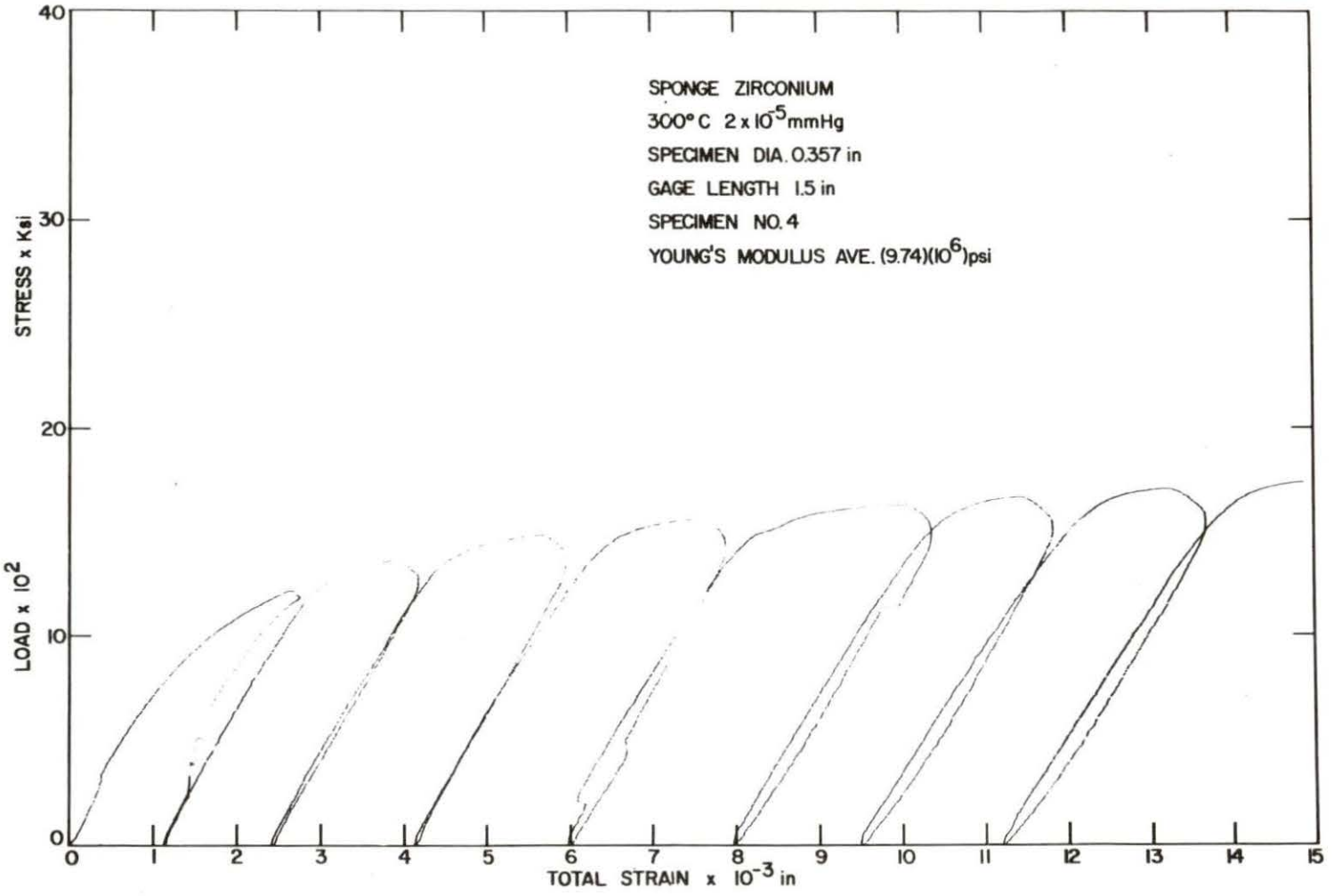


Fig. 15. Recording of cyclic loading in tension of sponge zirconium

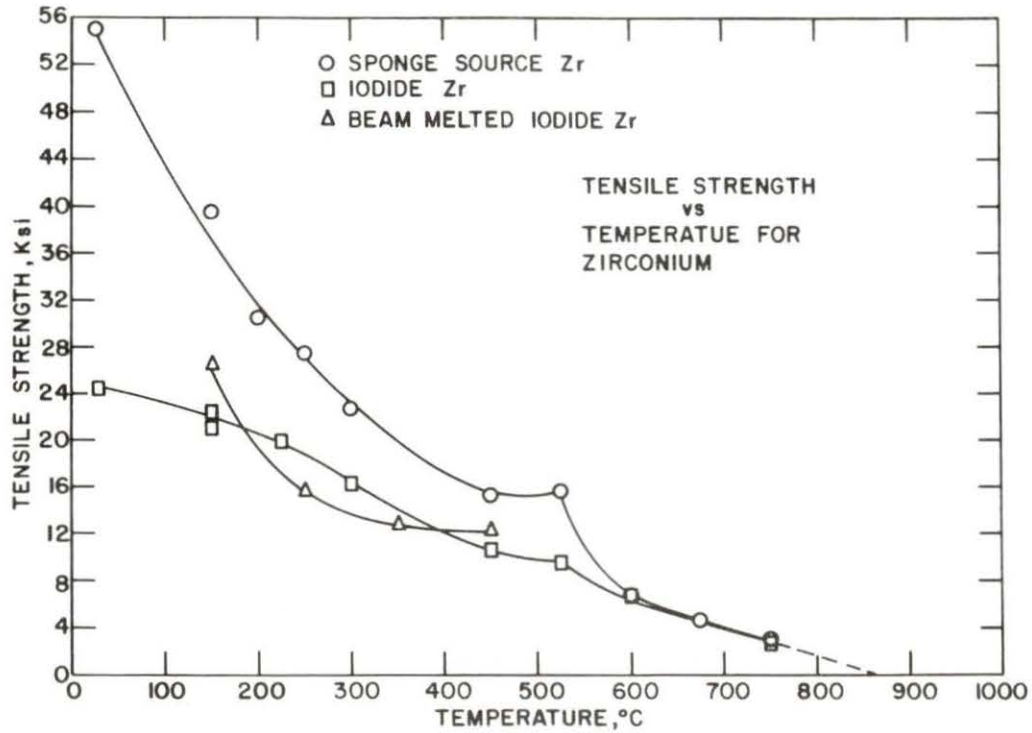


Fig. 16. Tensile strength vs. temperature for zirconium

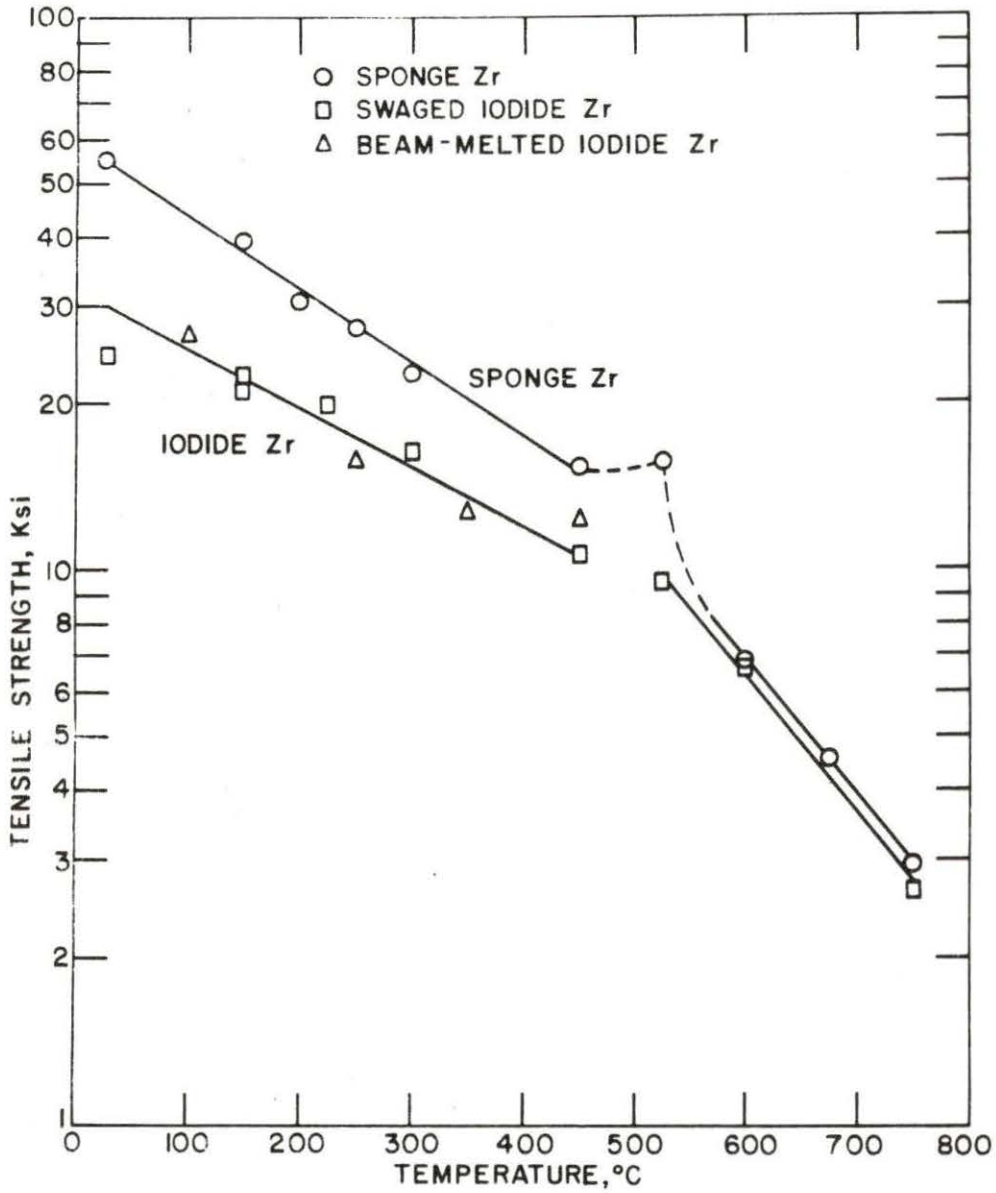


Fig. 17. Tensile strength vs. temperature for three types of zirconium

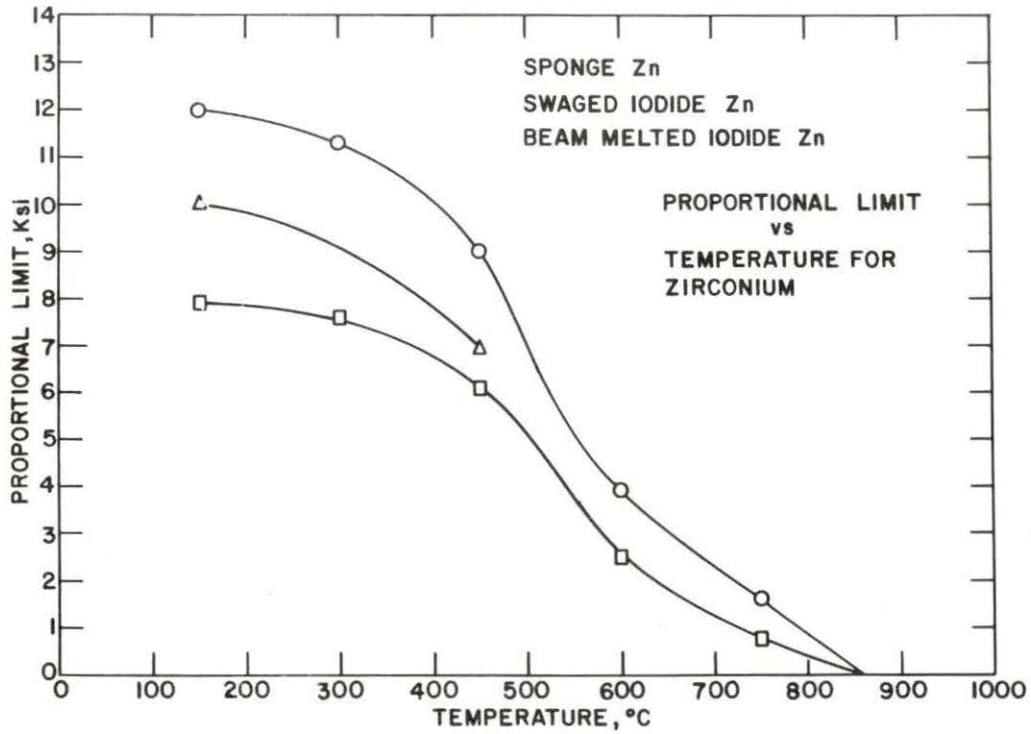


Fig. 18. Proportional limit vs. temperature for zirconium

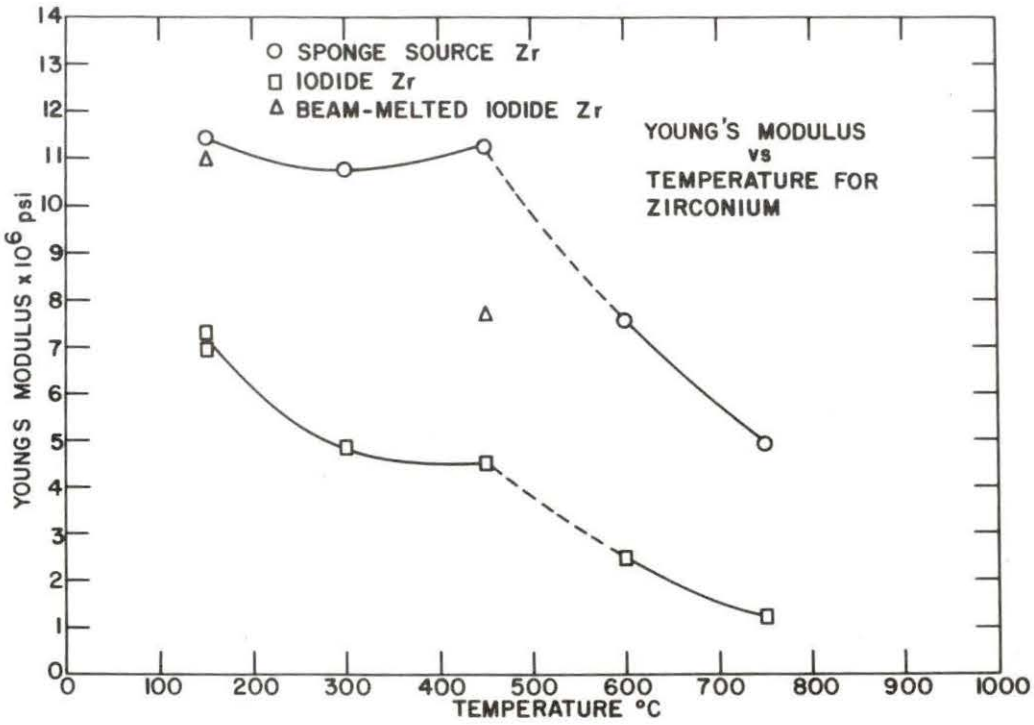


Fig. 19. Young's modulus vs. temperature for zirconium

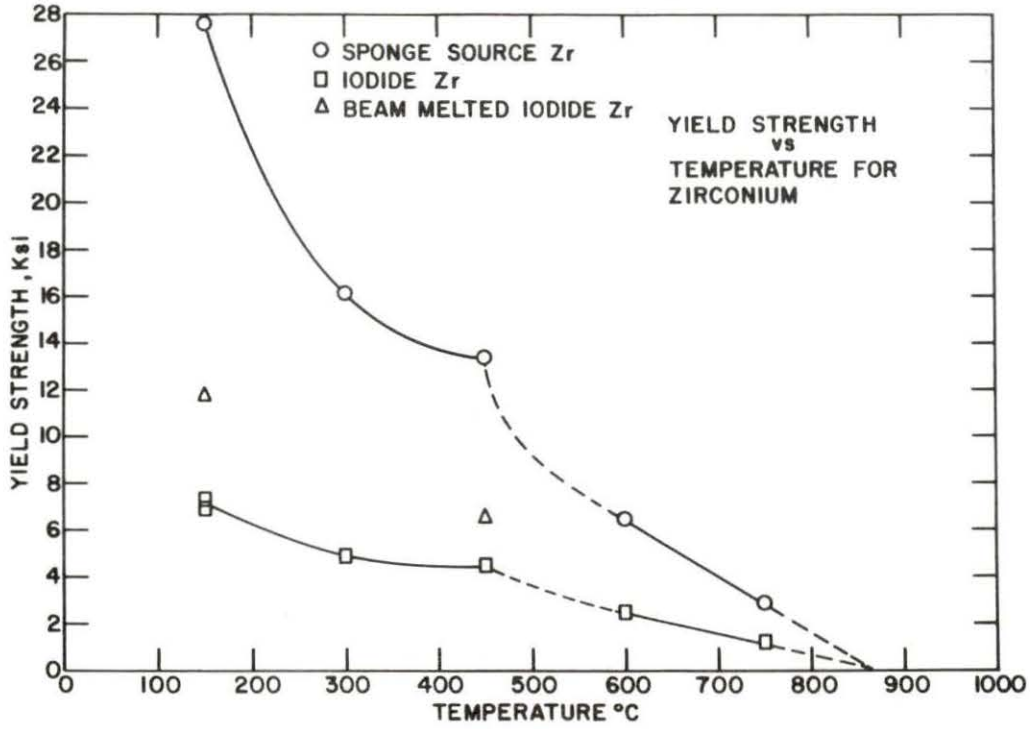


Fig. 20. Yield strength vs. temperature for zirconium

TABLE 2. Average Tensile and Fatigue Properties of Zr at Various Temperatures

Strain rate 0.025 in./in. min

| | Temperature °C | Tensile strength ksi | Young's Modulus psi x $10^6$ | Yield strength ksi | Proportional limit ksi | Endurance limit ksi | Fatigue ratio | Intercept $\log_e b$ | Slope - m | $S_y$ ** psi |
|---|---|---|---|---|---|---|---|---|---|---|
| Sponge source | 150 | 39.60 | 11.42 | 27.60 | 12.0 | 12.5 | 0.316 | 10.38 | 0.059 | 1,379 |
| Iodide | " | 22.00 | 12.30 | 7.10 | 7.9 | 8.8 | 0.400 | 10.20 | 0.086 | 491 |
| Beam-melted iodide | " | 26.40 | 10.96 | 11.75 | 10.0 | 11.1 | 0.420 | 10.04 | 0.046 | 528 |
| Sponge source | 300 | 22.70 | 10.76 | 16.15 | 11.3 | 11.8 | 0.520 | 10.27 | 0.055 | 1,172 |
| Iodide | " | 16.30 | 10.92 | 4.86 | 7.6 | 7.9 | 0.485 | 10.12* | 0.091* | 1,085 |
| Beam-melted iodide | " | | | | | | | | | |
| Sponge source | 450 | 15.30 | 11.22 | 13.40 | 9.0 | 8.7* | 0.569 | 10.19* | 0.068* | 1,380 |
| Iodide | " | 10.63 | 9.92 | 4.50 | 6.1 | 6.1 | 0.564 | 10.04* | 0.100* | 1,416 |
| Beam-melted iodide | " | 12.25 | 7.65 | 6.57 | 6.9 | 6.8 | 0.555 | 9.99 | 0.070 | 1,704 |
| Sponge source | 600 | 6.80 | 7.56 | 6.43 | 3.9 | 5.6 | 0.824 | 10.10 | 0.081 | 457 |
| Iodide | " | 6.72 | 7.60 | 2.48 | 2.5 | 3.8* | 0.565 | 9.92* | 0.104* | |
| Beam-melted iodide | " | | | | | | | | | |
| Sponge source | 750 | 2.94 | 4.91 | 2.88 | 1.6 | 2.4* | 0.816 | 9.84 | 0.090 | 321 |
| Iodide | " | 2.65 | 4.17 | 1.21 | 0.75 | 1.6* | 0.604 | 9.73 | 0.105 | 558 |
| Beam-melted iodide | " | | | | | | | | | |

* Interpolated from curve showing function vs. temperature.

** $S = bN^m \pm S_y$ psi.

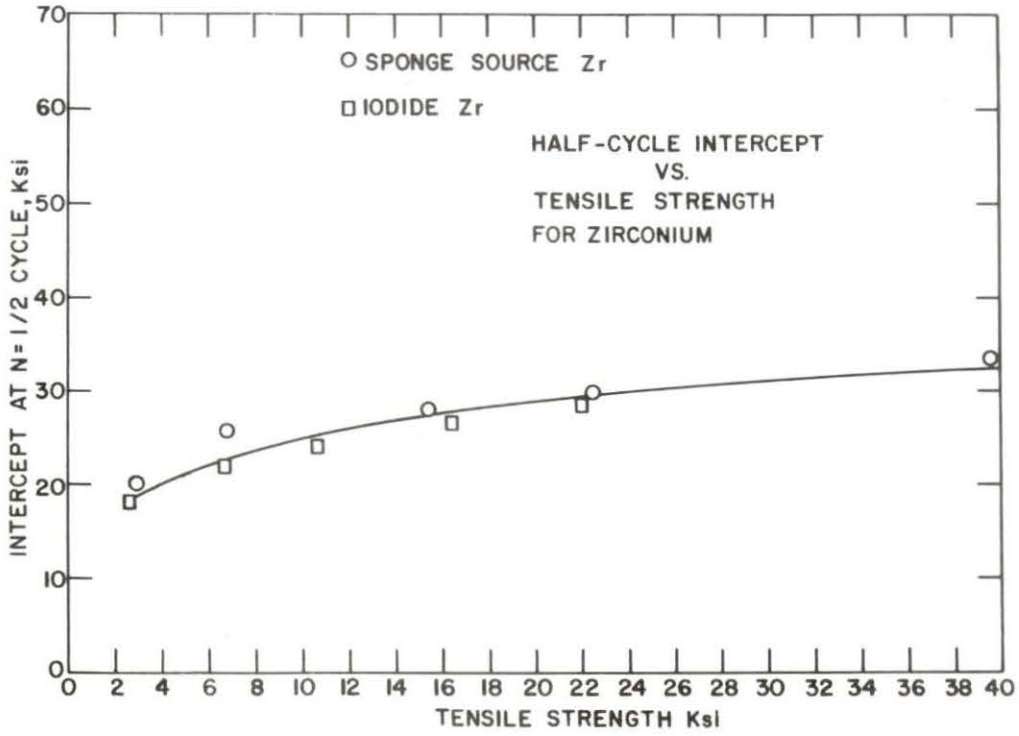


Fig. 21. Half-cycle intercept vs. tensile strength for zirconium

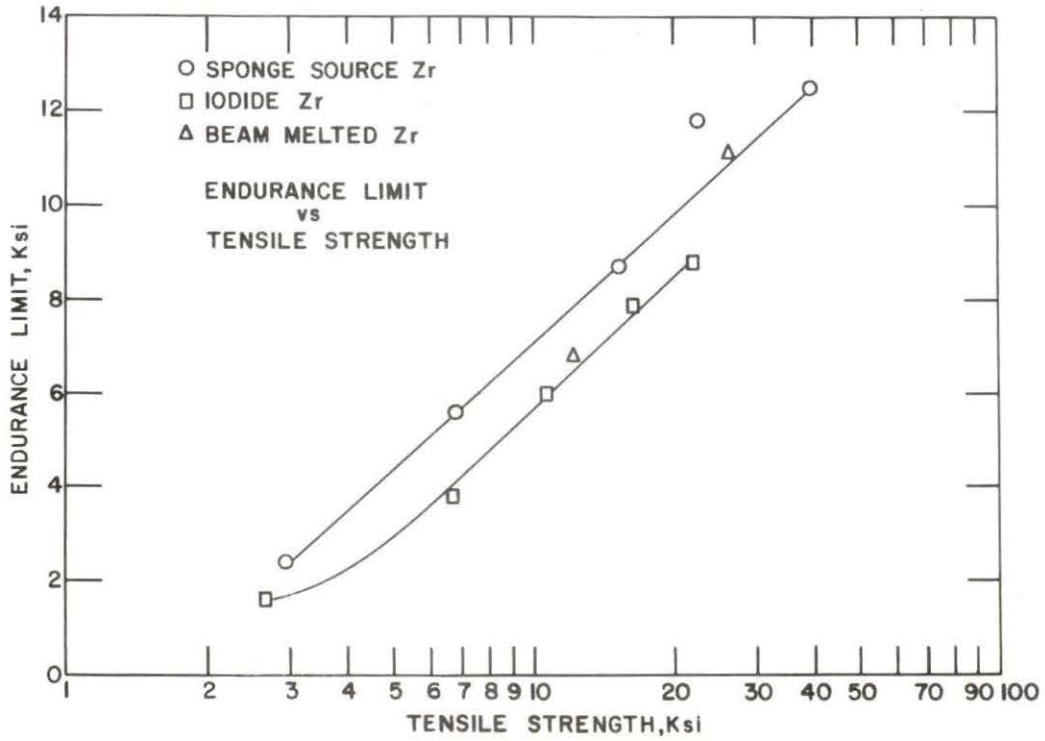


Fig. 22. Endurance limit vs. tensile strength

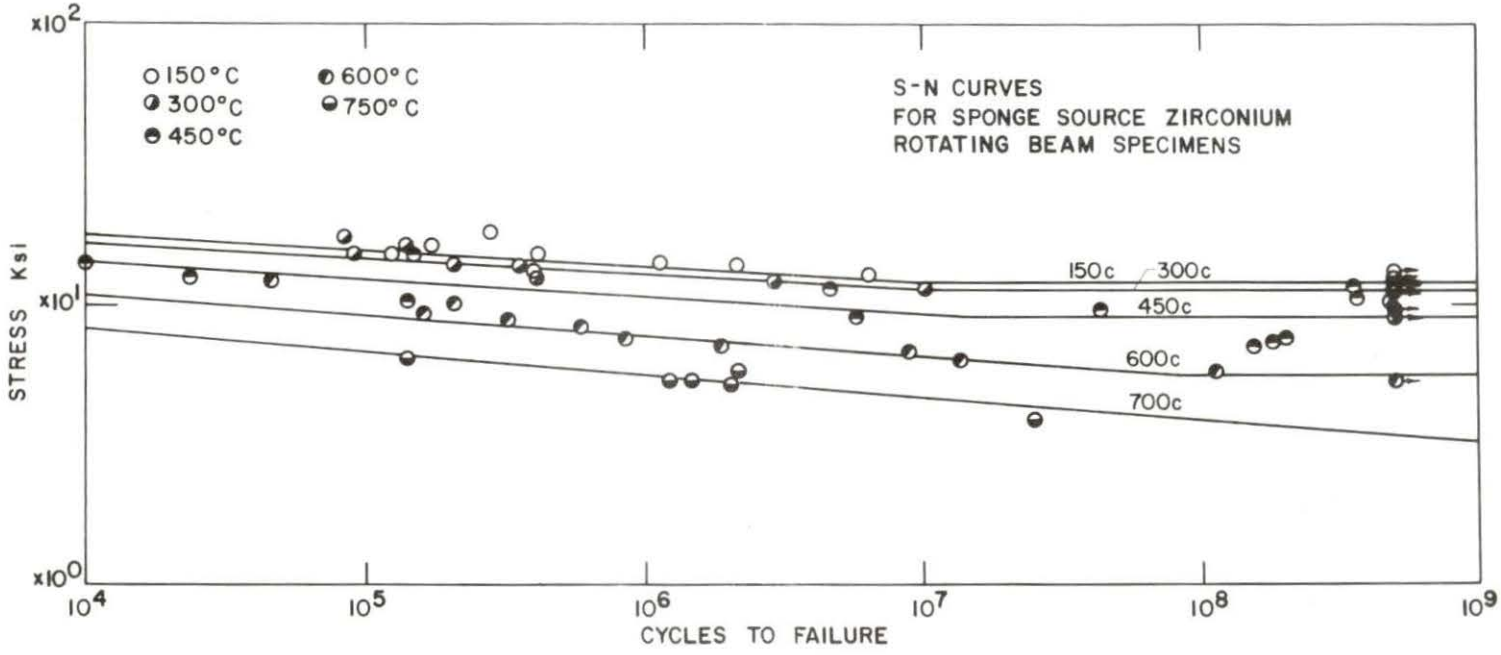


Fig. 23. Log S - N diagram for sponge zirconium

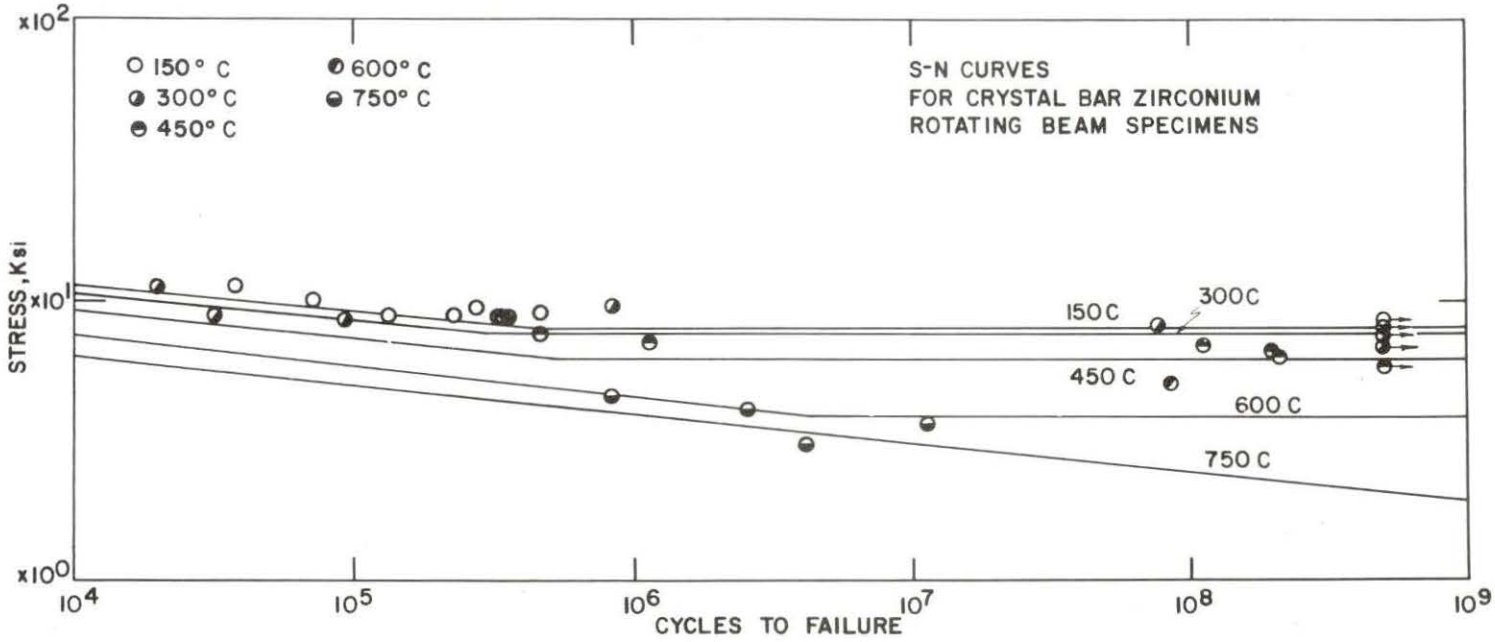


Fig. 24. Log S - N diagram for swaged and annealed iodide zirconium

## DISCUSSION

Zirconium transforms from a hexagonal close-packed structure to a body-centered cubic structure at approximately 862 C.

The various mechanical properties of zirconium decrease rapidly with temperature and it is interesting to note that they extrapolate to zero at approximately 862 C, and that all the curves meet at that temperature regardless of their values at lower temperatures (Figures 9, 16, 18). This indicates that as far as the structural usefulness of the metal is concerned, the transformation temperature may be considered to be the melting point (9, pp. 491-499). In this connection it should be noticed how widely the low temperature properties of the three test materials differ, so much in fact as to make them appear as distinct materials.

Early in the fatigue study it was noticed that a specimen being tested at 750 C would withstand for several million cycles a stress which was twice as high as the tensile strength of the material at the same temperature. In order to investigate this phenomenon it was decided to run a static flexure test on a fatigue machine by gradually applying a load and recording both the load and the deflection, the latter being measured with an LVDT. The stresses were calculated from $S = \frac{Mc}{I}$ and the strains for stresses below the proportional limit from $\epsilon = \frac{Mc}{EI}$. The calculated strains were compared with the measured deflection and it was assumed that for small angles the strain and the

deflection would be proportional. Above the proportional limit the strains were then calculated from the deflections. The results were plotted as a stress-strain curve, and was found to correspond with the one obtained from an ordinary tensile test.

The test was repeated twice with the specimen rotating at different speeds, and it was found that in both of these cases $\frac{d^2\sigma}{d\epsilon^2}$ was positive (Fig. 4).

The conclusion reached from this test is that the tensile strength depends on the rate of load application at least at the higher temperatures where creep is a factor.

Creep takes place in a metal due to dislocations that move within the crystal lattice and interact with it. The dislocations are produced from dislocation sources by the application to the metal of a stress which is sufficiently high to activate a dislocation. A dislocation will move through the lattice until it meets a barrier which it does not have energy to overcome; however, the addition of thermal energy may allow it to continue until it either meets another dislocation or some other barrier.

The nature of the creep process shows that it requires time to produce macroscopic strains and that the lower the temperature the more time is required. Therefore, when a specimen is loaded rapidly such as is the case with a rotating fatigue specimen the material does not have time to creep and in addition some of the dislocations may cancel each other because the load is continuously reversed.

The fatigue curves for all three types of zirconium show some scatter, which is especially large for the 450 C test temperature. Other properties show deviations at about the same temperature. For example, the tensile properties show discontinuities from 450 C to 525 C. Holmes (6, p. 11) shows that the activation energy for creep of Zircaloy-2 has a large peak at 350 C when the material is subjected to a stress of 20,000 psi; a lower stress would cause the peak to occur at a higher temperature. The knee which is found at a fairly constant number of cycles up to 450 C occurs much later above that temperature. Since there is no transformation in the metal the rapid change in properties occuring around 450 C must be due to recrystallization which does not occur in zirconium below temperatures of 400 C (9, pp. 394-400).

Photomicrographs of specimens tested below and above this temperature (Figs. 25, 26) are evidence that recrystallization takes place. Figure 25 shows specimens tested in tension for a relatively short time. The specimens tested above 400 C show the presence of many subgrains which are absent in the one tested below 400 C. Figure 26 shows specimens tested in fatigue for a relatively long time. The two tested below 400 C show the presence of some dislocations but the grains are all of approximately the same size. The specimen tested at 450 C indicates that the dislocations have become the nuclei for numerous subgrains, and the specimen tested at 750 C shows the effect of prolonged strain-cycling at a high temperature on the grain size.

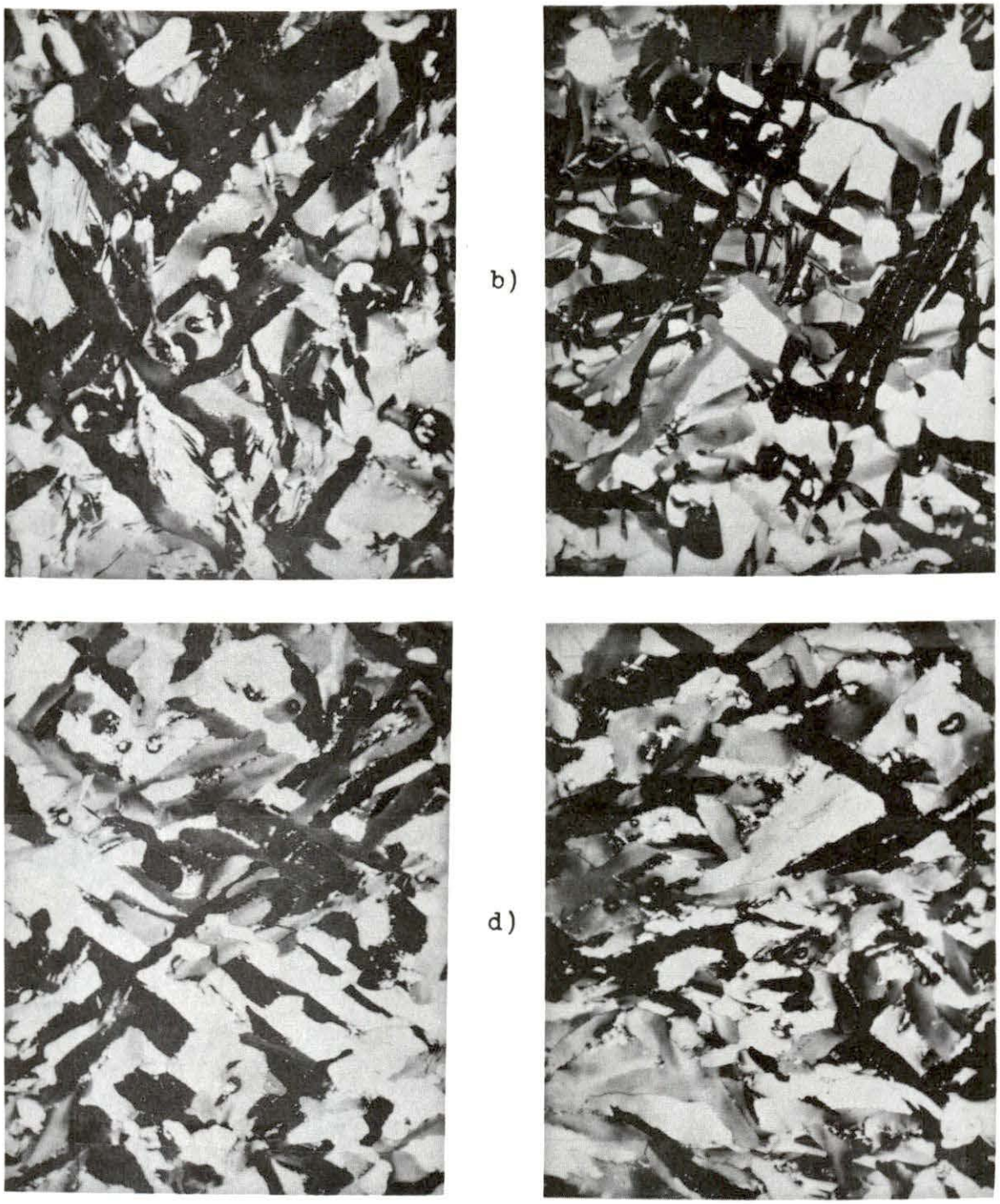


Fig. 25. Photomicrographs of sponge-source zirconium tested in tension at indicated temperatures

a) 300 C b) 450 C c) 525 C d) 600 C

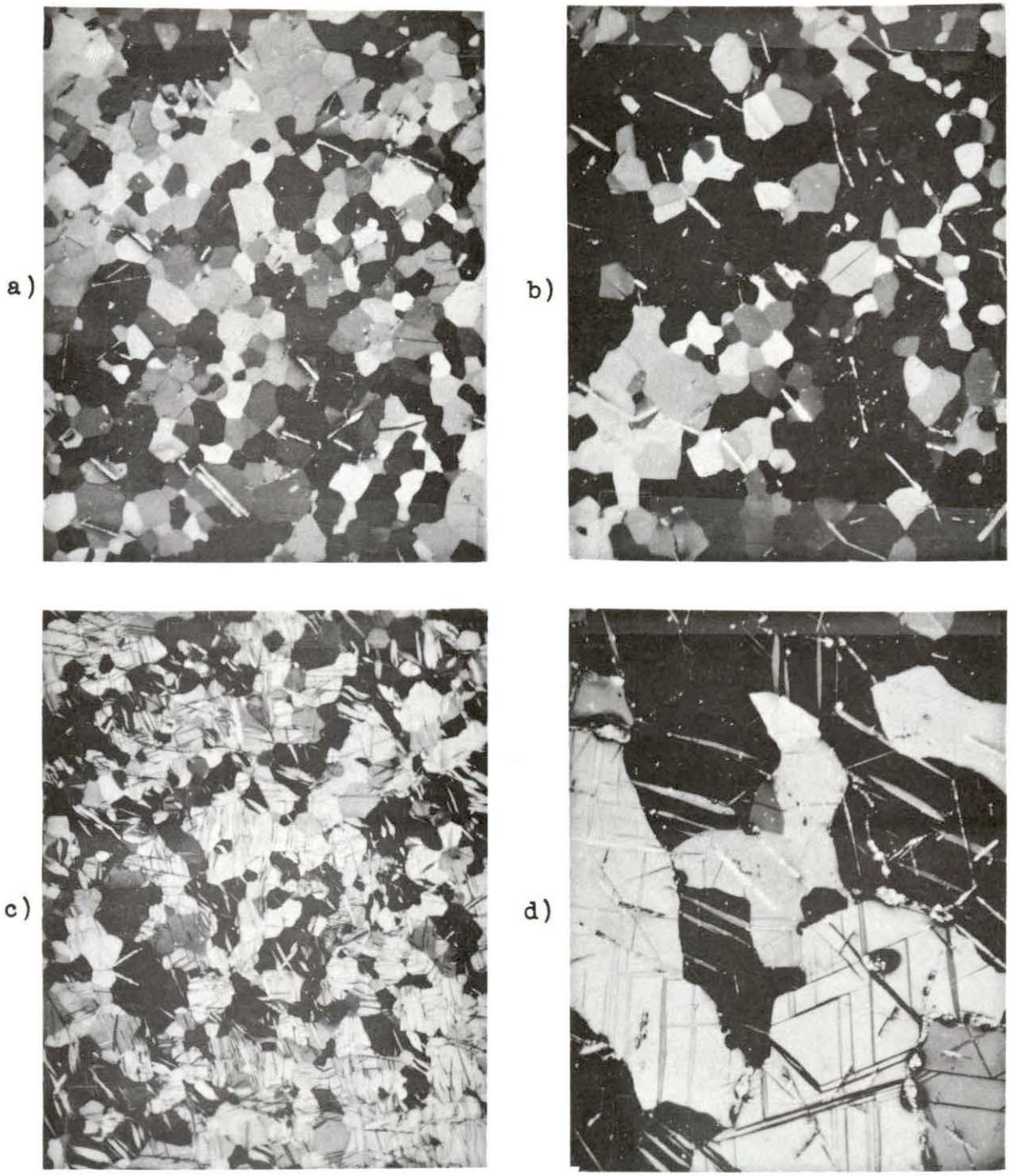


Fig. 26. Photomicrographs of swaged and annealed iodide zirconium tested in fatigue at indicated temperatures

a) 30 minutes @ 150 C
b) 189 minutes @ 300 C
c) 257 minutes @ 450 C
d) 185 minutes @ 750 C

In the plot of tensile strength vs. temperature (Fig. 16) the two iodide zirconiums are similar and show only about one-half the strength of sponge zirconium at room temperature. However, in the plot of endurance limit vs. temperature (Fig. 9) the beam-melted iodide zirconium appears much stronger than the swaged and annealed iodide zirconium and falls between it and the sponge zirconium. The reason for the large difference in the low-temperature tensile strength may be explained by the difference in the oxygen contents which is major difference in alloy content of the materials (Table 1). Accordingly, the endurance limits of the two iodide zirconiums should be similar and much smaller than the endurance limit of the sponge zirconium. Kearns and Mudge (8) did a study on the fatigue notch sensitivity of zirconium and zirconium alloys and found that oxygen or tin raised the unnotched fatigue strength by virtue of increasing the tensile strength, but had little effect on the notched fatigue strength.

It is evident from Figures 9 and 16 that the same tensile strength does not necessarily mean the same endurance limit for two different preparations of zirconium. This may also be seen from Figure 22 where endurance limit is plotted as a function of tensile strength for sponge and swaged iodide zirconium. If the endurance limit were a function of the tensile strength alone, all of the points should fall on a single curve regardless of the material, instead they fall on two distinct, almost parallel lines, one for each of the two materials.

Microscopic analysis of the swaged and annealed crystal bar showed no inhomogeneieties in this material, and a comparison of photomicrographs showed that the grains were approximately the same size, and with no visual evidence of residual stresses.

When the materials were annealed, the beam-melted iodide zirconium was brought above the transformation temperature and furnace cooled, whereas the swaged iodide zirconium was brought to a temperature below the transformation temperature and was cooled at a controlled rate.

The effect of beta-quenching is to raise the strength properties and decrease the ductility. The increase in yield strength is the most pronounced, while the change in tensile strength is slight for high purity zirconium (9, pp. 505-508). The results obtained from the tensile tests show that this is exactly what happened to the properties of the beam-melted, and it may therefore be concluded that it was beta-quenched.

Further proof of the beta-quench is that whereas the swaged and annealed iodide zirconium appeared smooth at the conclusion of a tensile test, the beam-melted zirconium had an "orange peel" surface which is indicative of previous large beta grains. If the S - N curves are extrapolated back to a half cycle, the stress which would produce failure in a half cycle would result. This quantity, the half-cycle intercept, has no physical significance since one cannot speak of fatigue failure when the material has been strained only once. Figure 21 shows the

half-cycle intercept vs. the tensile strength, and here there seems to be no distinction between the types of zirconium because all points fall along one line, indicating that for a short fatigue life the tensile strength is a good criterion of the relative fatigue strength.

Figures 12 and 13 are stress-strain diagrams of swaged and annealed iodide zirconium and of beam-melted iodide zirconium respectively. It appears from these curves that although the ultimate tensile strengths of the two materials are similar, the proportional limits, the moduli of elasticity, and the yield strengths are quite different, and that in fact these properties of the beam-melted iodide zirconium fall between the respective properties of swaged iodide zirconium and sponge zirconium just as did the endurance limits. The implication of this is that one of these properties might be used to determine the endurance limit.

If a tensile specimen is cycled through a few cycles of loading and unloading, and if the material is strain hardenable, the proportional limit will gradually increase until a fairly constant value has been reached. If the specimen is not stressed above the proportional limit there will be no hysteresis loop, and the energy absorbed by the specimen upon loading will be released upon unloading. If this were the case the specimen could be cycled at the proportional limit indefinitely, and the endurance limit would be equal to the proportional limit.

When the stress-cycling takes place at elevated temperatures the effect of annealing will play a role in the fatigue life. Wheeler and Gordon (17, pp. 1-5) in their study on copper found that the total energy released during annealing was larger when a material had been subjected to reversed deformation than if it had been subjected to unidirectional deformation. Thus, it is possible that the rearrangement of the dislocations taking place during repeated reversed deformation, together with an elevated temperature that allows movement of the dislocations and cancellation of those of opposite sign, would allow the material to be stressed indefinitely above the proportional limit, and that the amount above the proportional limit would increase with increasing temperature due to the increased mobility of the dislocations.

This effect is evident from Table 2 where the values of endurance limits and "proportional limit" may be compared. These values show that up to 450 C the two are very similar. Above that temperature, however, the endurance limit is much higher than the proportional limit, and this is expected because recrystallization, and therefore annealing, does not occur below 400 C.

If the knee is caused by strain aging its position should be temperature dependent. Figure 10 shows that at 300 C the knee position for the swaged and annealed iodide zirconium appears after a minimum number of cycles. Below and above this temperature it appears at a later number of cycles.

The reason for the later occurrence of the knee at lower temperatures may be that the interstitials which can act to pin the dislocations have lower mobility and that it takes them more time to diffuse to a localized slip region to induce pinning. At high temperatures the interstitials are so mobile as to cause no significant force on the dislocation (15, pp. 12-13) and strain hardening will therefore show its effect much later until at some temperature it disappears, and the material will no longer exhibit an endurance limit.

Although the half-cycle intercept has no physical significance, the fact that the same plot of half-cycle intercept vs. tensile strength seems to be representative of the metal regardless of the alloy content means that since the curve has been established for zirconium in general the tensile strength may be used to establish one point on the S - N curve.

The endurance limit may be estimated from the proportional limit obtained from repeated loadings in tension. The value of the endurance limit together with the occurrence of the knee will establish another point on the S - N curve, which may then be drawn by joining the two points on log paper with a straight line.

It should be noted that in order to obtain the proportional limit with sufficient accuracy it is necessary to use a large magnification of strain. The tests reported here were directly recorded as load vs. strain with a strain magnification of 1000.

## SUMMARY AND CONCLUSIONS

Fatigue and tensile tests were performed on three types of zirconium at temperatures ranging from 27 C to 750 C.

Tensile properties are presented in tabular form and are shown as stress-strain diagrams.

Fatigue properties are presented as S - N curves and their empirical equations; some fatigue properties are also shown as functions of tensile properties.

The following conclusions can be reached concerning the properties of zirconium.

1. Addition of oxygen increases the strength. An increase in the oxygen content from 30 ppm to 1290 ppm doubled the tensile strength at room temperature, but had less effect at increasing temperatures.

2. The strength decreases rapidly with increasing temperature and falls to zero at 862 C which is the alpha to beta transformation temperature.

3. Although the melting point of zirconium is 1845 C the transformation temperature should be considered as the melting point as far as the mechanical properties are concerned.

4. Zirconium exhibits an endurance limit which up to 450 C may be approximated by the proportional limit obtained from cyclic tensile loadings.

5. The tensile properties of zirconium are sensitive to rate of loading at elevated temperatures; it is thus necessary to specify the strain rate with any given tensile strength.

## SUGGESTIONS FOR FURTHER STUDY

Due to the important role played by the endurance limit in the design of many structures and the laborious manner in which it is usually obtained it would be interesting and profitable to investigate further the relationship between the endurance limit and the proportional limit as obtained from cyclic tensile loadings.

It is believed that for materials which have the property of strain-aging, and therefore exhibit a knee in the S - N curve, the two have a definite relationship.

## LITERATURE CITED


1. Bohn, J. R. Fatigue characteristics of uranium. Unpublished M.S. thesis. Ames, Iowa, Library, Iowa State University of Science and Technology. 1958.

2. Bohn, J. R. and Glenn Murphy. A high-temperature vacuum extensometer. U.S. Atomic Energy Commission Report IS-167 (Iowa State University of Science and Technology, Ames. Inst. for Atomic Research). 1960.

3. Coffin, L. F., Jr. A study of the effects of cyclic thermal stresses on a ductile metal. American Society of Mechanical Engineers Transactions 76:931-950. 1954.

4. Coffin, L. F., Jr. and J. H. Read. A study of the strain cycling and fatigue behaviour of a cold-worked metal. London, Institution of Mechanical Engineers. 1956.

5. Grover, H. J., S. A. Gordon and L. R. Jackson. Fatigue of metals and structures. U.S. Atomic Energy Commission Report NAVAER 00-25-543 (Office of the Chief of Naval Operations, Washington, D. C.). 1954.

6. Holmes, J. J. The activation energies for creep of Zircaloy-2. U.S. Atomic Energy Commission Report HW-70151 (Hanford Atomic Products Operation, Richland, Wash.). 1962.

7. Introduction to metals for elevated temperature use. U.S. Atomic Energy Commission Report DMIC 160 (Battelle Memorial Institute, Defence Metals Information Center, Columbus, Ohio). 1961.

8. Kearns, F. F. and W. L. Mudge. Fatigue notch sensitivity of zirconium and zirconium alloys. U.S. Atomic Energy Commission Report WAPD-88 (Westinghouse Electric Corporation, Atomic Power Division, Pittsburgh, Pa.). 1953.

9. Lustman, Benjamin and F. F. Kerze. The metallurgy of zirconium. New York, N.Y., McGraw-Hill Publishers. 1955.

10. Machlin, E. S. Dislocation theory of the fatigue of metals. National Advisory Committee for Aeronautics Technical Note 1489. 1948.

11. Mott, N. F. Theory of work-hardening of metal crystals. Philosophical Magazine 43:912-914. 1952.

12. Orowan, E. Theory of the fatigue of metals. London Royal Society Proceedings Ser. A, 171:79-105. 1939.

13. Pedersen, Knud and Glenn Murphy. Effects of temperature on mechanical properties of normal uranium dingot. U.S. Atomic Energy Commission Report IS-400 (Iowa State University of Science and Technology, Ames. Inst. for Atomic Research). 1962.

14. Polakowski, N. H. and A. Palchoudhuri. Softening of certain cold-worked metals under the action of fatigue loads. American Society for Testing Materials Proceedings 54:701-702. 1954.

15. Rally, F. C. and G. N. Sinclair. Influence of strain aging on the shape of the S - N diagram. University of Illinois Department of Theoretical and Applied Mechanics T&AM Report No. 87. 1955.

16. Swindeman, R. W. and D. A. Douglas. The failure of structural metals subjected to strain-cycling conditions. U.S. Atomic Energy Commission Report ORNL-2619 (Oak Ridge National Laboratory, Oak Ridge, Tenn.). 1958.

17. Wheeler, F. A., Jr. and Paul Gordon. The effect of reversed deformation on the stored energy released from copper during recovery and recrystallization. Illinois Institute of Technology Department of Metallurgical Engineering Office of Naval Research Report No. 5. 1960.

ACKNOWLEDGMENT

The author wishes to thank Dr. Glenn Murphy, Head of the Nuclear Engineering Department, for his valuable aid and criticism during the work on this investigation.

Thanks are also due the members of Nuclear Engineering Group I, Ames Laboratory, in particular Mr. Myron Willey for his help in polishing the fatigue specimens.